Circulation Research
JOURNAL OF THE AMERICAN HEART ASSOCIATION

AKT2 Confers Protection Against Aortic Aneurysms and Dissections

Ying H. Shen, Lin Zhang, Pingping Ren, Mary T. Nguyen, Sili Zou, Darrell Wu, Xing Li Wang, Joseph S. Coselli and Scott A. LeMaire

Circ Res. 2013;112:618-632; originally published online December 18, 2012;
doi: 10.1161/CIRCRESAHA.112.300735
Circulation Research is published by the American Heart Association, 7272 Greenville Avenue, Dallas, TX 75231

Print ISSN: 0009-7330. Online ISSN: 1524-4571

AKT2 Confers Protection Against Aortic Aneurysms and Dissections

Ying H. Shen, Lin Zhang, Pingping Ren, Mary T. Nguyen, Sili Zou, Darrell Wu, Xing Li Wang, Joseph S. Coselli, Scott A. LeMaire

Rationale: **Aortic aneurysm and dissection (AAD) are major diseases of the adult aorta caused by progressive medial degeneration of the aortic wall. Although the overproduction of destructive factors promotes tissue damage and disease progression, the role of protective pathways is unknown.**

Objective: **In this study, we examined the role of AKT2 in protecting the aorta from developing AAD.**

Methods and Results: **AKT2 and phospho-AKT levels were significantly downregulated in human thoracic AAD tissues, especially within the degenerative medial layer. *Akt2*-deficient mice showed abnormal elastic fibers and reduced medial thickness in the aortic wall. When challenged with angiotensin II, these mice developed aortic aneurysm, dissection, and rupture with features similar to those in humans, in both thoracic and abdominal segments. Aortas from *Akt2*-deficient mice displayed profound tissue destruction, apoptotic cell death, and inflammatory cell infiltration that were not observed in aortas from wild-type mice. In addition, angiotensin II–infused *Akt2*-deficient mice showed significantly elevated expression of matrix metalloproteinase-9 (MMP-9) and reduced expression of tissue inhibitor of metalloproteinase-1 (TIMP-1). In cultured human aortic vascular smooth muscle cells, AKT2 inhibited the expression of MMP-9 and stimulated the expression of TIMP-1 by preventing the binding of transcription factor forkhead box protein O1 to the *MMP-9* and *TIMP-1* promoters.**

Conclusions: **Impaired AKT2 signaling may contribute to increased susceptibility to the development of AAD. Our findings provide evidence of a mechanism that underlies the protective effects of AKT2 on the aortic wall and that may serve as a therapeutic target in the prevention of AAD. (*Circ Res*. 2013;112:618-632.)**

Key Words: aortic aneurysm and dissection ■ AKT ■ forkhead box protein O1 ■ matrix metalloproteinase-9 ■ tissue inhibitor of metalloproteinase-1

Aortic aneurysm and dissection (AAD) are major diseases of the adult aorta.[1] Despite significant improvements in the diagnosis and surgical repair of AAD, the rate of morbidity and mortality from aortic rupture remains high, particularly when the disease involves the thoracic aorta.[1] Understanding the pathogenesis of AAD is necessary to develop a better treatment for these conditions.

In This Issue, see p 575

The key histopathologic feature of aortic aneurysm is progressive degeneration of the medial layer of the aortic wall, which is characterized by the loss of smooth muscle cells (SMCs) and the destruction of extracellular matrix (ECM).[2,3] These events lead to progressive dilatation of the vascular wall and AAD formation, ultimately resulting in lethal aortic rupture. Pharmacological prevention is ineffective, largely because the molecular mechanisms responsible for the vascular degeneration underlying AAD formation are poorly understood.

The activation of stress signaling pathways and the subsequent production of tissue-destructive factors, such as matrix metalloproteinases (MMPs), promote aortic aneurysm formation and progression. However, there may be native protective systems that counterbalance destructive factors to maintain a healthy vascular wall. When these protective mechanisms are impaired, the uninhibited tissue-destructive factors may drive excessive aortic destruction and lead to AAD formation. Although destructive factors that function in the pathogenesis of AAD have been well documented, protective mechanisms remain to be identified.

The multifunctional AKT signaling pathway, which is activated by insulin, growth factors, and cytokines, is implicated in a diverse range of cellular functions, including cell metabolism, survival, proliferation, and migration.[4] AKT has

Original received July 30, 2012; revision received December 11, 2012; accepted December 18, 2012. In November 2012, the average time from submission to first decision for all original research papers submitted to *Circulation Research* was 15.8 days.

From the Division of Cardiothoracic Surgery, Michael E. DeBakey Department of Surgery, Baylor College of Medicine, Houston, Texas; and Texas Heart Institute at St. Luke's Episcopal Hospital, Houston, Texas.

The online-only Data Supplement is available with this article at http://circres.ahajournals.org/lookup/suppl/doi:10.1161/CIRCRESAHA.112.300735/-/DC1.

Correspondence to Scott A. LeMaire, Baylor College of Medicine, One Baylor Plaza, BCM 390, Houston, TX 77030 (e-mail slemaire@bcm.edu); or Dr Ying H. Shen, Baylor College of Medicine, One Baylor Plaza, BCM 390, Houston, TX 77030 (e-mail hyshen@bcm.edu).

Circulation Research **is available at http://circres.ahajournals.org** **DOI: 10.1161/CIRCRESAHA.112.300735**

Nonstandard Abbreviations and Acronyms

AAD	aortic aneurysm and dissection
AngII	angiotensin II
CA	constitutively active
DN	dominant negative
ECM	extracellular matrix
FOXO1	forkhead box protein O1
MMP	matrix metalloproteinase
shRNA	short hairpin RNA
siRNA	small interfering RNA
SMC	smooth muscle cell
TAA	thoracic aortic aneurysm
TAD	thoracic aortic dissection
TIMP	tissue inhibitor of metalloproteinase
TUNEL	terminal deoxynucleotidyltransferase dUTP nick-end labeling
VSMC	vascular smooth muscle cell
WT	wild type

profound effects on the cardiovascular system.[5] In the heart, the acute activation of AKT promotes cardiomyocyte survival and function,[6–8] whereas chronic AKT activation can cause cardiac hypertrophy and maladaptive remodeling.[9,10] In the vascular wall, the AKT pathway regulates endothelial NO synthase and vascular tone.[11] Inflammation[12] and metabolic stress[13] can impair AKT signaling, resulting in endothelial dysfunction. AKT signaling also promotes vascular SMC (VSMC) proliferation[14–16] and migration.[5,17] Although proliferative vascular remodeling can be harmful in neointimal hyperplasia and restenosis,[18] it may be beneficial in vascular repair and regeneration in AAD.

In this study, we observed significantly decreased AKT2 expression and AKT phosphorylation/activation in human AAD tissues. Therefore, we investigated whether AKT2 plays a protective role against AAD formation in the aortic wall in mice and examined the direct effects of AKT2 on matrix metalloproteinase-9 (MMP-9) and tissue inhibitor of metalloproteinase (TIMP)-1 expression in cultured aortic VSMCs. Our findings suggest that AKT2 has a protective role in the aorta and that AKT2 impairment may contribute to the development of AAD.

Methods

An expanded Methods section is available in the Online Data Supplement.

Human Tissue Studies

All protocols were approved by the institutional review board of Baylor College of Medicine. Informed consent was obtained from all enrolled patients. For this study, we used aortic tissues from 28 patients with descending thoracic AAD, including 12 with thoracic aortic aneurysm (TAA) without dissection (age, 66.8±4.7 years) and 16 with chronic thoracic aortic dissection (TAD; age, 63.6±5.1 years). Aortic tissues from 12 age-matched organ donors were used as controls (Online Table I). AKT levels and activation in these tissues were examined by Western blot and immunohistochemical analysis.

Animal Studies

All animal experiments were approved by the Institutional Animal Care and Use Committee at Baylor College of Medicine in accordance with the guidelines of the National Institutes of Health. Wild-type (WT; C57BL/6J) and *Akt2*$^{-/-}$ (B6.Cg-*Akt2*$^{tm1.1Mbb}$/J with C57BL/6J background) mice from The Jackson Laboratory (Bar Harbor, ME) were used. Eight-week-old male mice were infused with either saline or 1000 ng/min per kilogram angiotensin II (AngII) for 4 weeks. AAD incidence, aortic destruction, inflammatory cell infiltration, and MMP-9 and TIMP-1 expression were compared between *Akt2*$^{-/-}$ and WT mice.

Statistical Analysis

All quantitative data are presented as the mean±SD. Data were analyzed with SPSS software, version 11.0 (SPSS Inc, Chicago, IL). Normality of the data was examined by using the Kolmogorov–Smirnov test. Independent *t* tests were used to compare normally distributed values, and the Mann–Whitney test was used to compare data without a normal distribution. Multiple groups were compared by using 1-way analysis of variance or by using the Kruskal–Wallis test, as appropriate. For all statistical analyses, 2-tailed probability values were used.

Results

AKT2 and Active AKT Levels Are Significantly Reduced in the Medial Layer of Human AAD Tissue

We first examined AKT and active AKT levels in aortic tissues from patients with descending TAA and chronic TAD. Western blot analysis of AKT protein in the protein extracts of the whole aortic wall (ie, intima, media, and adventitia in TAA; media and adventitia in TAD; Figure 1A) showed that total AKT protein levels were significantly lower in TAA tissues (but not in TAD tissues) than in control tissues. Furthermore, whereas AKT1 protein levels were similar among groups, AKT2 protein levels were significantly lower in both TAA and TAD tissues than in control tissues. Importantly, phospho-AKT levels and phospho-AKT/total AKT ratios were significantly lower in both TAA and TAD tissues than in control tissues, indicating the reduced activation of AKT in human AAD.

Immunostaining analysis of AKT protein in the diseased aortic wall showed a pattern dependent on pathological changes (Figure 1B). Total AKT protein levels were high in the hyperplastic intima and adventitia, particularly in inflammatory cells and proliferating cells. In the media, although total AKT was abundantly expressed in preserved areas and in hyperplastic areas (ie, areas with increased cell density), it was expressed at substantially lower levels in the cells of degenerative areas (ie, areas with tissue destruction and markedly decreased cell density). Importantly, regardless of total AKT protein levels, phospho-AKT levels and phospho-AKT/total AKT ratios were significantly lower in the media of diseased aortas than in the media of control aortas (Figure 1C). Together, these observations indicate that AKT2 expression is reduced in human AAD tissues, particularly in the degenerative medial layer, and that AKT signaling in these tissues may have been impaired.

Akt2-deficient Mice Develop AAD When Challenged With AngII

To further determine whether impaired AKT2 expression contributes to the development of AAD, we examined AAD formation in *Akt2*$^{-/-}$ and WT mice. In the absence of exogenous stress, no *Akt2*$^{-/-}$ mice developed spontaneous AAD (Figure 2A and 2B). When mice were challenged with AngII, which has been shown to induce aortic aneurysms in *ApoE*$^{-/-}$ mice,[19]

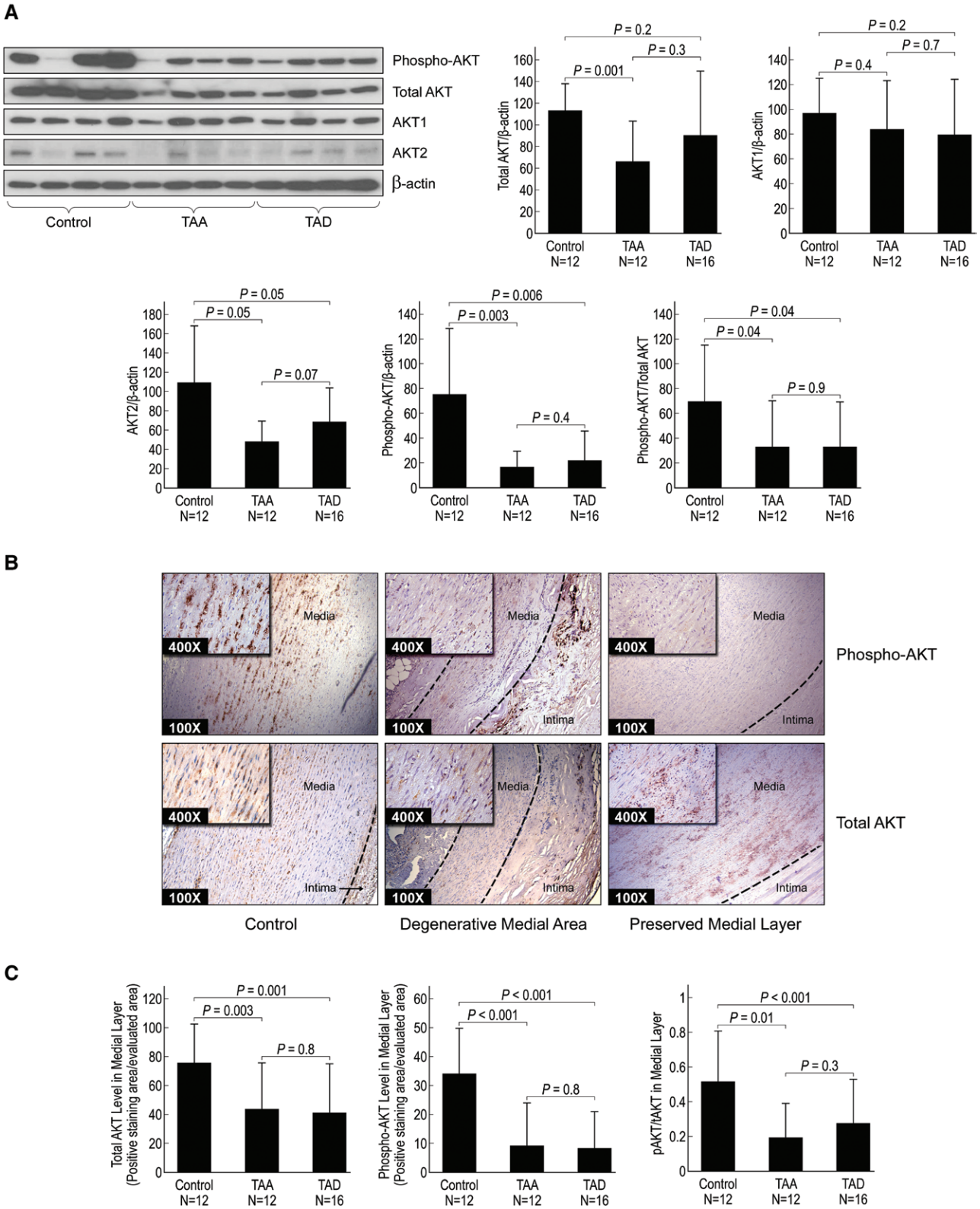

Figure 1. Decreased phospho-AKT levels in the aortic wall of human aortic aneurysm and dissection tissues. A, Phospho-AKT, total AKT, AKT1, and AKT2 proteins in human control aortas, thoracic aortic aneurysm (TAA) tissues, and thoracic aortic dissection (TAD) tissues were detected by Western blot by using anti–phospho-AKT (Ser 473) and anti-AKT antibodies. Representative blots and quantification of the mean intensities of phospho-AKT, total AKT, AKT1, and AKT2 bands (normalized with those of β-actin) show decreased levels of AKT2 and phospho-AKT, as well as decreased ratios of phospho-AKT/total AKT in aortas from TAA and TAD patients. **B**, Phospho-AKT (Ser 473) and total AKT proteins in control, TAA, and TAD tissues were detected by immunostaining. Representative images are shown. For each sample, the positive-staining areas for phospho-AKT and total AKT were measured in 5 randomly selected microscopic fields (magnification ×400) and normalized with the total number of cells/nuclei in the counted area. **C**, The mean normalized staining signals for phospho-AKT, total AKT, and the ratio of phospho-AKT to total AKT are shown.

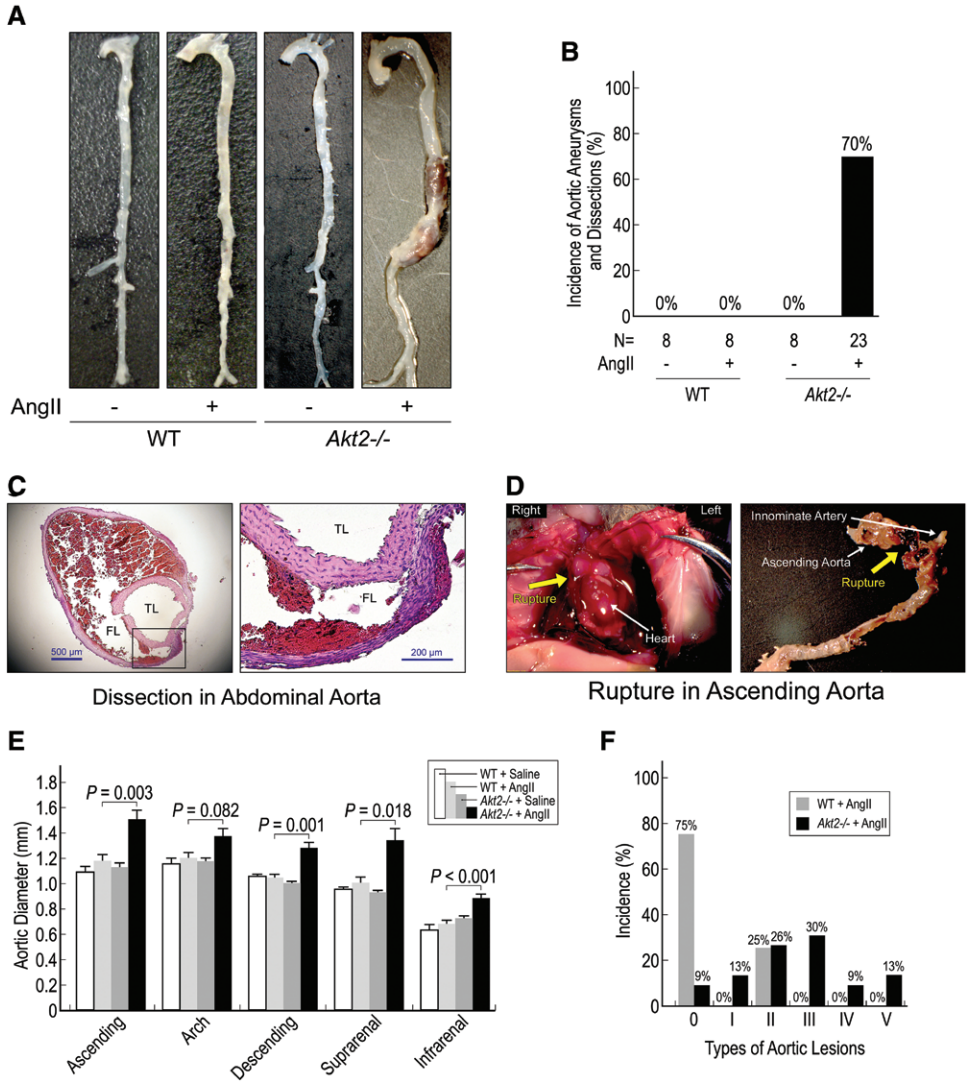

Figure 2. Development of aortic aneurysms and dissections in *Akt2*$^{-/-}$ mice infused with angiotensin II (AngII). Wild-type (WT) and *Akt2*$^{-/-}$ mice were infused with saline or AngII for 4 weeks. **A**, Representative excised aortas show that *Akt2*$^{-/-}$ mice challenged with AngII developed aneurysms involving the thoracic and abdominal aorta. **B**, The incidence of all aortic aneurysms and dissections in *Akt*$^{-/-}$ and WT mice (P<0.001). **C**, Histologically confirmed aortic dissection with a characteristic true lumen (TL) and false lumen (FL) in AngII-infused *Akt2*$^{-/-}$ mice. **D**, In an AngII-infused *Akt2*$^{-/-}$ mouse that suddenly died, median sternotomy (**left**) revealed that blood surrounded the heart and great vessels, which was caused by the rupture of an ascending aortic aneurysm (**arrow**; **right**). **E**, Comparison of aortic diameter among saline or AngII-infused WT and *Akt2*$^{-/-}$ mice. **F**, The types of aortic lesions, according to a modified classification system based on that of Daugherty et al,[19] are shown.

systolic blood pressure increased similarly in *Akt2*$^{-/-}$ mice and WT mice (Online Figure IA). In the thoracic and abdominal aorta of 70% of AngII-infused *Akt2*$^{-/-}$ mice, we observed aortic aneurysms (Figure 2A; aortic diameter >1.5× of the mean aortic diameter of saline-infused *Akt2*$^{-/-}$ mice), dissections (Figure 2C), or rupture (Figure 2D), whereas no AngII-infused WT mice developed aortic aneurysms (aortic diameter >1.5× of the mean aortic diameter of saline-infused WT mice) or dissections (P<0.001; Figure 2B). Furthermore, compared with AngII-infused WT mice, AngII-infused *Akt2*$^{-/-}$ mice showed significant increases in the diameter of most aortic segments (Figure 2E). When we characterized aortic gross pathology by using the classification of Daugherty et al,[19] we found that only 25% of AngII-infused WT mice developed aortic lesions (none of which were more severe than Type II), whereas 91% of AngII-infused *Akt2*$^{-/-}$ mice developed aortic lesions (P<0.001; 52% of which were more severe than Type II; Figure 2F). Furthermore, in AngII-infused *Akt2*$^{-/-}$ mice, vessel dilatation (aortic diameter >1.25× of the mean aortic diameter of saline-infused *Akt2*$^{-/-}$ mice) was observed most frequently in the suprarenal abdominal segment (74%), followed by the ascending (65%), descending thoracic (61%), arch (39%), and infrarenal (39%) aortic segments, 4 weeks after AngII infusion (Online Figure IB). Aneurysms in AngII-infused *Akt2*$^{-/-}$ mice were most frequently observed in the ascending (39%) and suprarenal abdominal (35%) aortic regions, followed by the descending thoracic (17%), arch (13%), and infrarenal (9%) aortic segments (Online Figure IC). Fatal rupture occurred in 13% of AngII-infused *Akt2*$^{-/-}$ mice, exclusively in the ascending aortic segment and

typically within 1 week after the initiation of AngII infusion (Online Figure ID). Together, our results show that AngII infusion led to severe aortic disease in the setting of *Akt2* deficiency, suggesting that AKT2 has protective role against the formation of AAD.

Elastic Fiber Destruction Is Significantly Increased in AngII-challenged *Akt2*$^{-/-}$ Mice

To characterize the histological changes in the aortas of *Akt2*$^{-/-}$ mice, we analyzed elastic lamellar architecture by using Verhoeff elastic staining. Compared with aortas from saline-infused WT mice, aortas from saline-infused *Akt2*$^{-/-}$ mice displayed notable abnormalities in aortic architecture, with thinner and straighter elastic fibers (Figure 3A), increased elastic fiber fragmentation (Figure 3B), and significantly reduced medial thickness (Figure 3C). When infused with AngII, *Akt2*$^{-/-}$ mice exhibited severe elastic fiber fragmentation (Figure 3B). These findings suggest that AKT2 may prevent AAD formation and progression by promoting and maintaining normal aortic structure and by inhibiting elastin destruction.

Apoptosis Is Significantly Increased in AngII-challenged *Akt2*$^{-/-}$ Mice

Because AKT plays an important role in cell survival, we analyzed apoptosis in the aortas of *Akt2*$^{-/-}$ and WT mice by using the terminal deoxynucleotidyl transferase dUTP nick-end labeling (TUNEL) assay. As shown in Figure 4A, TUNEL-positive cells were observed in AngII-infused WT mice but not in saline-infused WT mice. The number of TUNEL-positive cells was markedly increased in the aortic wall of saline-infused *Akt2*$^{-/-}$ mice but was even higher when *Akt2*$^{-/-}$ mice were challenged with AngII, particularly in the lesion regions. In addition, cleaved caspase 3 (Figure 4B) and apoptosis-inducing factor (Figure 4C) were detected in the aortas of AngII-infused *Akt2*$^{-/-}$ mice, suggesting the potential involvement of both caspase-dependent and caspase-independent apoptotic pathways.

Inflammatory Cell Infiltration Is Significantly Increased in AngII-challenged *Akt2*$^{-/-}$ Mice

We also examined the infiltration of the aorta by inflammatory cells, which have been shown to promote ECM degradation

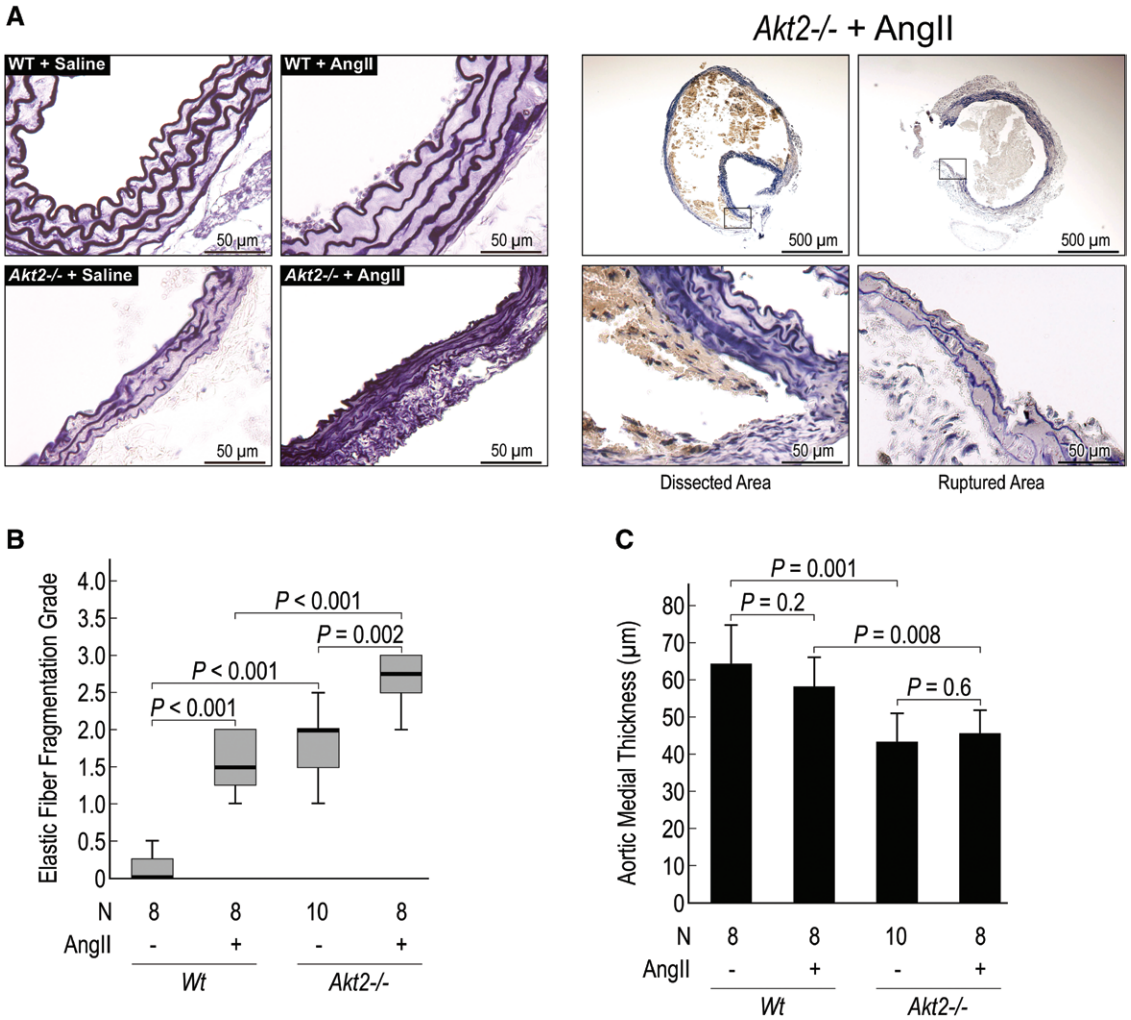

Figure 3. Significantly increased elastic fiber destruction and reduced medial thickness in angiotensin II (AngII)–infused *Akt2*$^{-/-}$ mice. A, Representative histological sections of the aorta (Verhoeff elastic staining) demonstrating abnormalities in elastic lamellar architecture in saline-infused *Akt2*$^{-/-}$ mice and marked elastin destruction in AngII-infused *Akt2*$^{-/-}$ mice. Comparisons of (**B**) elastic fiber fragmentation scores (Grade 0=none, Grade 1=minimal, Grade 2=moderate, and Grade 3=severe) and (**C**) medial thickness among groups are shown. WT indicates wild-type.

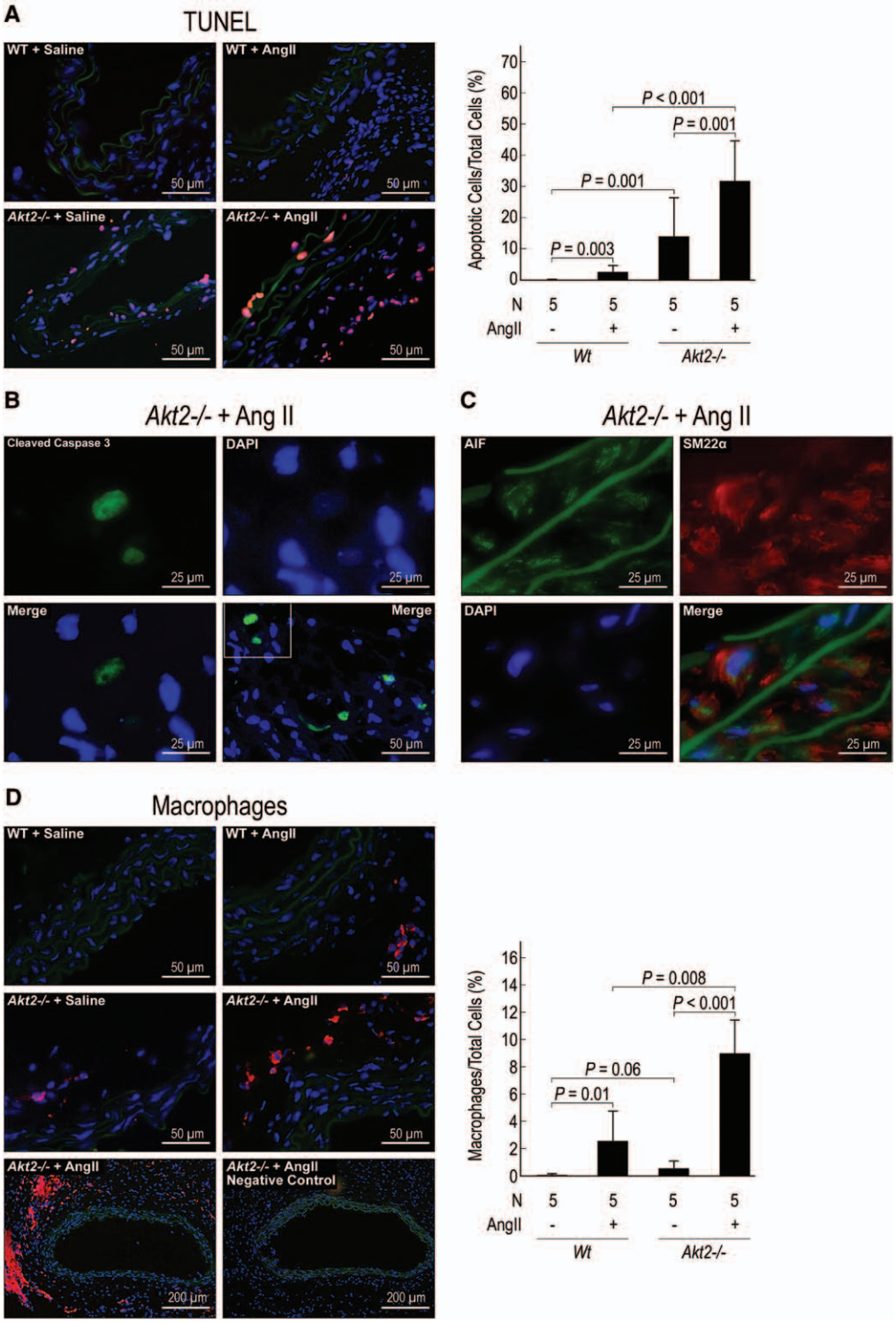

Figure 4. Significantly increased apoptosis and inflammatory cell infiltration in angiotensin II (AngII)-infused *Akt2*$^{-/-}$ mice. A, Representative terminal deoxynucleotidyl transferase dUTP nick-end labeling (TUNEL)-stained images and comparison of the number of TUNEL-positive cells normalized to the total number of cells are shown. The number of TUNEL-positive cells was significantly increased in the lesion areas of AngII-infused *Akt2*$^{-/-}$ mice, particularly in dissected areas. Cleaved caspase 3 (**B**) and apoptosis-inducing factor (AIF) (**C**) were detected in the aortas of AngII-infused *Akt2*$^{-/-}$ mice. **D**, Representative images of immunofluorescence staining and quantification (mean positive-staining area normalized with evaluated aortic area) of CD68-positive macrophages in the aortic wall show a significant increase in macrophages in AngII-infused *Akt2*$^{-/-}$ mice. WT indicates wild-type. DAPI indicates 4',6-diamidino-2-phenylindole.

and cell injury. In the absence of AngII infusion, the infiltration of macrophages (marked by the presence of CD68; Figure 4D) and CD3-positive T cells (Online Figure II) was minimal in the aortas of saline-infused WT mice and *Akt2*$^{-/-}$ mice. In the presence of AngII, the infiltration of these cells was observed within the aortic wall of WT mice and *Akt2*$^{-/-}$ mice. However,

AngII-challenged *Akt2*$^{-/-}$ mice had significantly more inflammatory cell infiltration that was even more pronounced in areas of tissue destruction and dissection (Figure 4D). Most of the macrophages in the aortic tissue of AngII-challenged *Akt2*$^{-/-}$ mice were observed in the adventitia. Macrophages were also detected in the media-adventitia boundary area, and a few macrophages were identified in the media of the aortic wall.

MMP-9 Expression Is Increased and TIMP-1 Expression Is Decreased in AngII-challenged *Akt2*$^{-/-}$ Mice

To further investigate the potential mechanisms for increased elastin destruction in *Akt2*$^{-/-}$ mice, we examined the expression of MMP-9 and MMP-2, which are key proteinases in ECM protein destruction. We found that the levels of MMP-9 protein (Figure 5A) and mRNA (Online Figure IIIA) and MMP-2 protein (Online Figure IIIB) were significantly increased in the aortic media and adventitia of AngII-challenged *Akt2*$^{-/-}$ mice, particularly in lesion segments. In these mice, MMP-9 was expressed in CD68-positive macrophages (Figure 5B) and in SM22α-positive SMCs (Figure 5C; Online Figure IIIC). In the aortic media, SMCs seemed to produce more MMP-9 than did macrophages (Figure 5B and 5C), suggesting that MMP-9 from SMCs may play a critical role in medial destruction and aortic dysfunction.

In addition, TIMP-1 protein (Figure 5D) and mRNA (Online Figure IIID) levels were increased in AngII-infused WT mice, saline-infused *Akt2*$^{-/-}$ mice, and AngII-infused *Akt2*$^{-/-}$ mice. Double immunostaining showed the colocalization of TIMP-1 and MMP-9 (Figure 5E) in the aortic wall, indicating that increased TIMP-1 expression may represent a protective response to increased MMP expression and aortic injury. However, the induction of TIMP-1 was lower (Figure 5D) and the MMP-9/TIMP-1 ratio was significantly higher (Figure 5E) in AngII-infused *Akt2*$^{-/-}$ mice than in AngII-infused WT mice, indicating an insufficient counterbalance of MMP-9 with TIMP-1 in AngII-infused *Akt2*$^{-/-}$ mice.

Consistent with these findings, the results of in situ gelatin zymography showed increased MMP activity in the aortic media of AngII-infused *Akt2*$^{-/-}$ mice (Figure 5F), suggesting that MMP-9 and MMP-2 production by SMCs may play an important role in medial destruction.

AKT2 Inhibits MMP-9 Expression and Enhances TIMP-1 Expression in Cultured Aortic VSMCs

To further investigate the mechanism of the AKT2-mediated regulation of MMP-9 and TIMP-1, we examined the effects of AKT2 on MMP-9 and TIMP-1 protein and mRNA expression in human aortic VSMCs. Whereas the overexpression of WT-AKT2 reduced MMP-9 and increased TIMP-1 protein levels, the short hairpin RNA (shRNA)-mediated knockdown of AKT2 increased MMP-9 and decreased TIMP-1 protein levels (Figure 6A). Furthermore, quantitative real-time polymerase chain reaction results showed that WT-AKT2 significantly reduced *MMP-9* and increased *TIMP-1* mRNA levels, whereas *AKT2* shRNA increased *MMP-9* and decreased *TIMP-1* mRNA levels (Figure 6B). Our data suggest that AKT2 inhibits MMP-9 expression and enhances TIMP-1 expression at the mRNA level.

Forkhead Box Protein O1 Positively Regulates MMP-9 and Negatively Regulates TIMP-1 Expression in Human Aortic VSMCs

To further investigate the potential mechanism for the AKT2-mediated regulation of MMP-9 and TIMP-1 expression, we examined whether the transcription factor forkhead box protein O1 (FOXO1), a major downstream target of AKT that can be phosphorylated and inactivated by AKT, regulates the expression of MMP-9 and TIMP-1. WT-FOXO1 but not dominant negative (DN)-FOXO1 or *FOXO1* small interfering RNA increased MMP-9 protein levels (Figure 7A), and WT-FOXO1 and constitutively active (CA) FOXO1, but not DN-FOXO1, increased *MMP-9* mRNA levels (Figure 7B), indicating that FOXO1 positively regulates MMP-9 expression.

In contrast to the positive regulation of MMP-9 expression by FOXO1, we found that TIMP-1 expression is negatively regulated by FOXO1. WT-FOXO1 decreased TIMP-1 protein levels, whereas DN-FOXO1 or *FOXO1* small interfering RNA increased TIMP-1 protein levels (Figure 7A). In addition, WT-FOXO1 and CA-FOXO1, but not DN-FOXO1, decreased *TIMP-1* mRNA levels (Figure 7B).

FOXO1 Binds to the Promoters of *MMP-9* and *TIMP-1* in Human Aortic VSMCs

Promoter sequence analysis of the 5′-flanking region of the human *MMP-9* gene showed the presence of 3 potential binding sites for FOXO transcription factors (Figure 7C). By using the ChIP assay, we showed that WT-FOXO1 and CA-FOXO1, but not DN-FOXO1, bind to FOXO binding site 2 of *MMP-9* (Figure 7D). FOXO1 also bound to sites 1 and 3 (data not shown). Our data suggest that the binding of FOXO1 to FOXO binding sites on the *MMP-9* promoter may be critical for FOXO1-mediated stimulation of *MMP-9* gene expression.

Promoter sequence analysis of the 5′-flanking region of the human *TIMP-1* gene showed the presence of 5 potential binding sites for FOXO transcription factors. Interestingly, one of the FOXO binding sites we identified and subsequently tested in the *TIMP-1* promoter is in close proximity to a binding site for GATA transcription factor 1 (GATA1) (Figure 7E). GATA1 is a transcription factor that is phosphorylated by AKT and mediates AKT-induced TIMP-1 expression.[20] We performed ChIP analysis to examine the binding of FOXO1 and GATA1 to the *TIMP-1* promoter and found that WT-FOXO1 and CA-FOXO1 increased FOXO1 binding while decreasing GATA1 binding to the *TIMP-1* promoter, whereas DN-FOXO1 decreased FOXO1 binding while increasing GATA1 binding to the *TIMP-1* promoter (Figure 7F). The inverse relationship between FOXO1 and GATA1 binding to the *TIMP-1* promoter suggests that FOXO1 binding to this site may prevent GATA1 from binding to the *TIMP-1* promoter, resulting in the suppression of *TIMP-1* transcription.

AKT2 Regulates MMP-9 and TIMP-1 by Inhibiting FOXO1

We examined whether AKT2 regulates MMP-9 expression by regulating FOXO1-mediated MMP-9 and TIMP-1

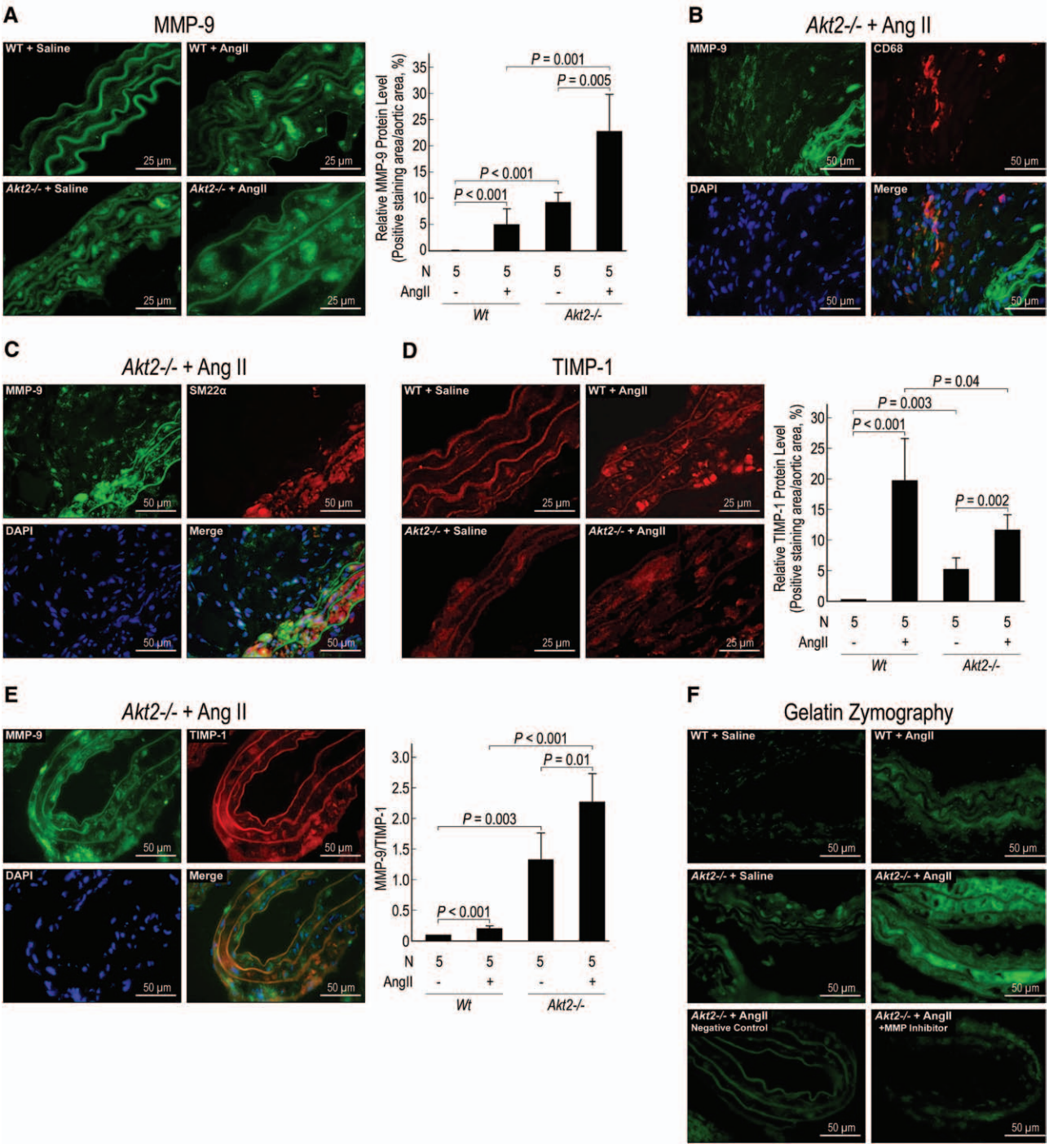

Figure 5. Significantly increased matrix metalloproteinase (MMP)-9 expression and MMP-9/tissue inhibitor of metalloproteinase (TIMP)-1 ratio in angiotensin II (AngII)-infused *Akt2*$^{-/-}$ mice. A, Representative images of immunofluorescence staining and quantification of the mean positive-staining area normalized with the evaluated aortic area show increased MMP-9 expression in aortas from AngII-infused *Akt2*$^{-/-}$ mice. Double staining for MMP-9 and CD68 or MMP-9 and SM22α shows increased MMP-9 expression in (**B**) CD68-positive macrophages and in (**C**) SM22α-positive SMCs in the aortas of AngII-infused *Akt2*$^{-/-}$ mice. **D**, Representative images of immunofluorescence staining and quantification of TIMP-1 expression (the mean positive-staining area normalized with the evaluated area) shows lower TIMP-1 expression in aortas from AngII-infused *Akt2*$^{-/-}$ mice than in AngII-infused wild-type (WT) mice. **E**, Double staining for MMP-9 and TIMP-1 in an aorta from an AngII-infused *Akt2*$^{-/-}$ mouse. Comparison shows increased MMP-9/TIMP-1 ratios in aortas from AngII-infused *Akt2*$^{-/-}$ mice. **F**, Representative zymography images show increased MMP activity in aortas from AngII-infused *Akt2*$^{-/-}$ mice. DAPI indicates 4',6-diamidino-2-phenylindole.

expression. We found that WT-AKT2 prevented the FOXO1-induced stimulation of MMP-9 protein and mRNA expression, whereas *AKT2* shRNA amplified the FOXO1-induced stimulation of MMP-9 protein and mRNA expression (Figure 8A and 8B). ChIP analysis showed that WT-AKT2 reduced the binding of FOXO1 to the *MMP-9* promoter, whereas *AKT2* shRNA increased the binding of FOXO1 to the *MMP-9* promoter (Figure 8C). Furthermore, WT-AKT2

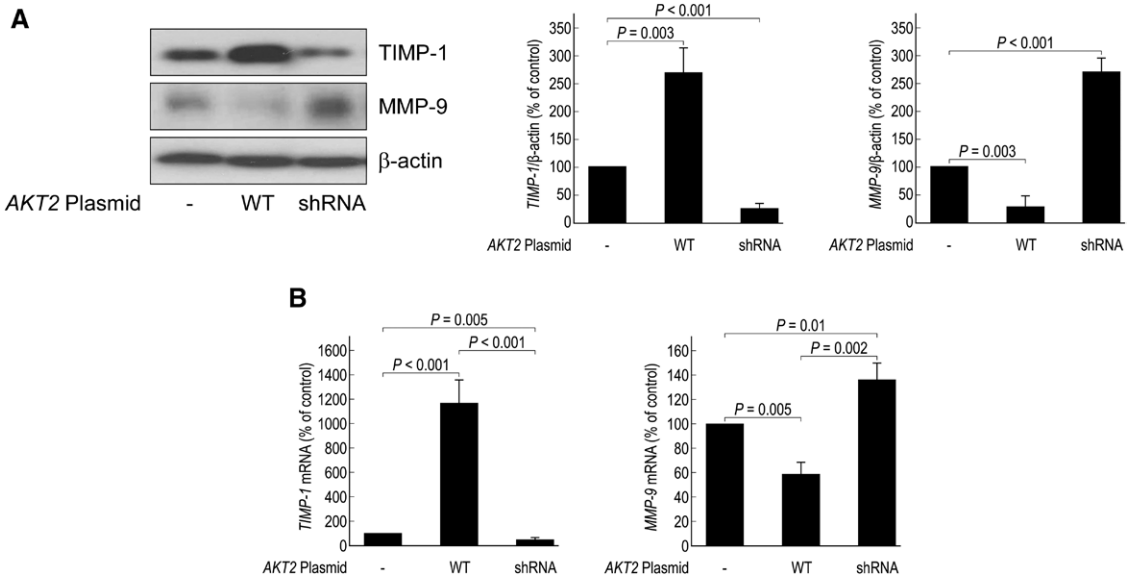

Figure 6. Effects of AKT2 on tissue inhibitor of metalloproteinase (TIMP)-1 and matrix metalloproteinase (MMP)-9 expression. **A**, Western blot analysis of TIMP-1 and MMP-9 protein levels in aortic vascular smooth muscle cells (VSMCs) that were transfected with wild-type *AKT2* (WT-*AKT2*) or *AKT2* short hairpin RNA (shRNA). Representative blots from 3 independent experiments are shown. Quantification of the mean intensities of TIMP-1 and MMP-9 bands (normalized with those of β-actin) are shown. **B**, *TIMP-1* and *MMP-9* mRNA levels were examined by reverse transcription and quantitative real-time polymerase chain reaction in VSMCs transfected with WT-*AKT2* or *AKT2* shRNA. *TIMP-1* and *MMP-9* mRNA expression was normalized with that of β-actin and is expressed as the percentage of the control. Data represent the mean±SD (n=3).

prevented WT-FOXO1 from binding to the *MMP-9* promoter, whereas WT-AKT2 failed to prevent CA-FOXO1 from binding to the *MMP-9* promoter, indicating that the inhibition of FOXO1 by AKT2 is FOXO1-phosphorylation dependent.

In addition, WT-AKT2 prevented the FOXO1-induced inhibition of TIMP-1 protein and mRNA expression, whereas *AKT2* shRNA amplified the FOXO1-induced inhibition of TIMP-1 protein and mRNA expression (Figure 8A and 8B). WT-AKT2 also reduced the binding of FOXO1 to the *TIMP-1* promoter, whereas *AKT2* shRNA increased the binding of FOXO1 to the *TIMP-1* promoter (Figure 8D). In contrast, WT-AKT2 induced GATA1 binding to the *TIMP-1* promoter, whereas AKT2 shRNA reduced GATA1 binding to the TIMP-1 promoter (Figure 8D). The inability of WT-AKT2 to prevent CA-FOXO1 from binding to the *TIMP-1* promoter indicates that the inhibition of FOXO1 by AKT2 is FOXO1-phosphorylation dependent.

We also showed that AKT2 inhibits FOXO1 action by preventing its nuclear translocation (Figure 8E). Silencing AKT2 expression with *AKT2* small interfering RNA or inhibiting AKT activation with Wortmannin promoted the nuclear translocation of FOXO1 (Figure 8E). Furthermore, consistent with our in vitro observations, high levels of FOXO1 protein were observed in the nucleus of aortic SMCs in AngII-infused *Akt2*$^{-/-}$ mice (Figure 8F), suggesting the activation of FOXO1 in these cells. Moreover, a significant amount FOXO1 protein was also observed in the aortic media in human TAA tissue (Figure 8G).

Together, these data suggest that AKT2 may inhibit MMP-9 expression by preventing FOXO1-mediated *MMP-9* transcription and that AKT2 may stimulate TIMP-1 expression by inhibiting FOXO1 and stimulating GATA1-regulated *TIMP-1* transcription (Online Figure IV).

Discussion

In this study, we have identified a novel molecular mechanism for AKT2 in protecting against the formation of AAD. Following our initial observation that AKT2 protein and AKT activation were reduced in human thoracic AAD, we then showed that *Akt2* deficiency in mice markedly increased susceptibility to AngII-induced AAD formation. Furthermore, we found that AKT2 suppressed MMP-9 expression and stimulated TIMP-1 expression by inhibiting FOXO1 in cultured human aortic VSMCs. Our results suggest that impaired AKT2 signaling in the aorta may increase susceptibility to AAD.

Although *Akt2*$^{-/-}$ mice did not develop spontaneous AAD in the absence of exogenous stress, the aortas of these mice showed significant abnormalities. These results suggest that AKT2 may play a critical role in the response to hemodynamic stress. Furthermore, when challenged with AngII, 70% of *Akt2*$^{-/-}$ mice, but not WT mice, developed marked aortic dilatation with aneurysm formation, dissection, and rupture, with features similar to those seen in human aortic disease. Thus, we speculate that AKT2 activation may protect the aortic wall against aneurysm formation in response to stress. Our results support the notion that, in addition to the well-known overactivation of destructive forces, native protective mechanisms are in place that counterbalance destructive forces to maintain vascular wall integrity.

Several mechanisms may account for AKT2's protective effects. One possible mechanism through which AKT2 may protect against the formation of aortic aneurysms is by promoting

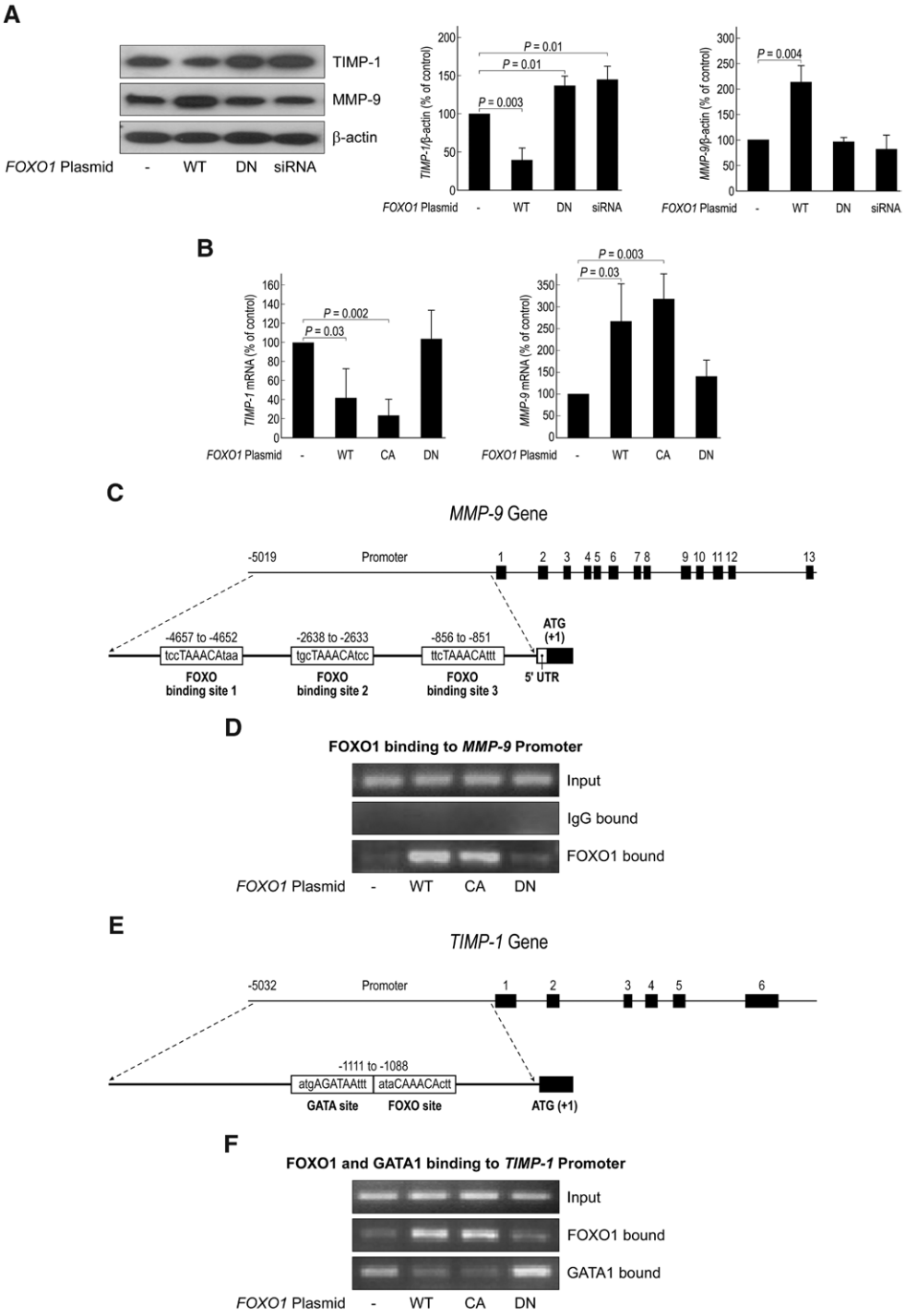

Figure 7. The effects of forkhead box protein O1 (FOXO1) on matrix metalloproteinase (MMP)-9 and tissue inhibitor of metalloproteinase (TIMP)-1 expression. Aortic vascular smooth muscle cells (VSMCs) were transfected with plasmids expressing wild-type (WT)-*FOXO1*, constitutively active (CA)-*FOXO1*, dominant negative (DN)-*FOXO1*, or *FOXO1* small interfering RNA, and (**A**) MMP-9 and TIMP-1 protein expression was examined by Western blot. Representative blots from 3 independent experiments are shown. Quantification of the mean intensities of TIMP-1 and MMP-9 bands (normalized with those of β-actin) is shown. **B**, *MMP-9* and *TIMP-1* mRNA levels were examined by reverse transcription and quantitative real-time polymerase chain reaction (PCR) and were normalized with levels of β-actin mRNA. Levels of mRNA are expressed as the percentage of the control. Data represent the mean±SD (n=3). **C**, Diagram showing the location of FOXO binding sites in the human *MMP-9* promoter. **D**, Chromatin immunoprecipitation (ChIP) analysis showing that FOXO1 bound to FOXO binding site 2 of the *MMP-9* promoter in aortic VSMCs transfected with WT-*FOXO1* and CA-*FOXO1* but not DN-*FOXO1*. FOXO1–DNA complexes were cross-linked by formaldehyde and immunoprecipitated with anti-FOXO1 antibody. Sites in the *MMP-9* promoter bound by FOXO1 were detected by PCR and normalized with input DNA. Representative blots from 2 independent experiments are shown. **E**, Diagram showing the location of FOXO and GATA transcription factor 1 (GATA1) binding sites in the human *TIMP-1* promoter. **F**, ChIP analysis showing that FOXO1 bound to the *TIMP-1* promoter in aortic VSMCs transfected with WT-*FOXO1* and CA-*FOXO1* but not DN-*FOXO1*. FOXO1–DNA complexes were cross-linked and immunoprecipitated with anti-FOXO1 antibody and anti-GATA1 antibody. Sites in the *TIMP-1* promoter bound by FOXO1 and GATA1 were detected by PCR and normalized with input DNA. Representative blots from 2 independent experiments are shown. UTR indicates untranslated region.

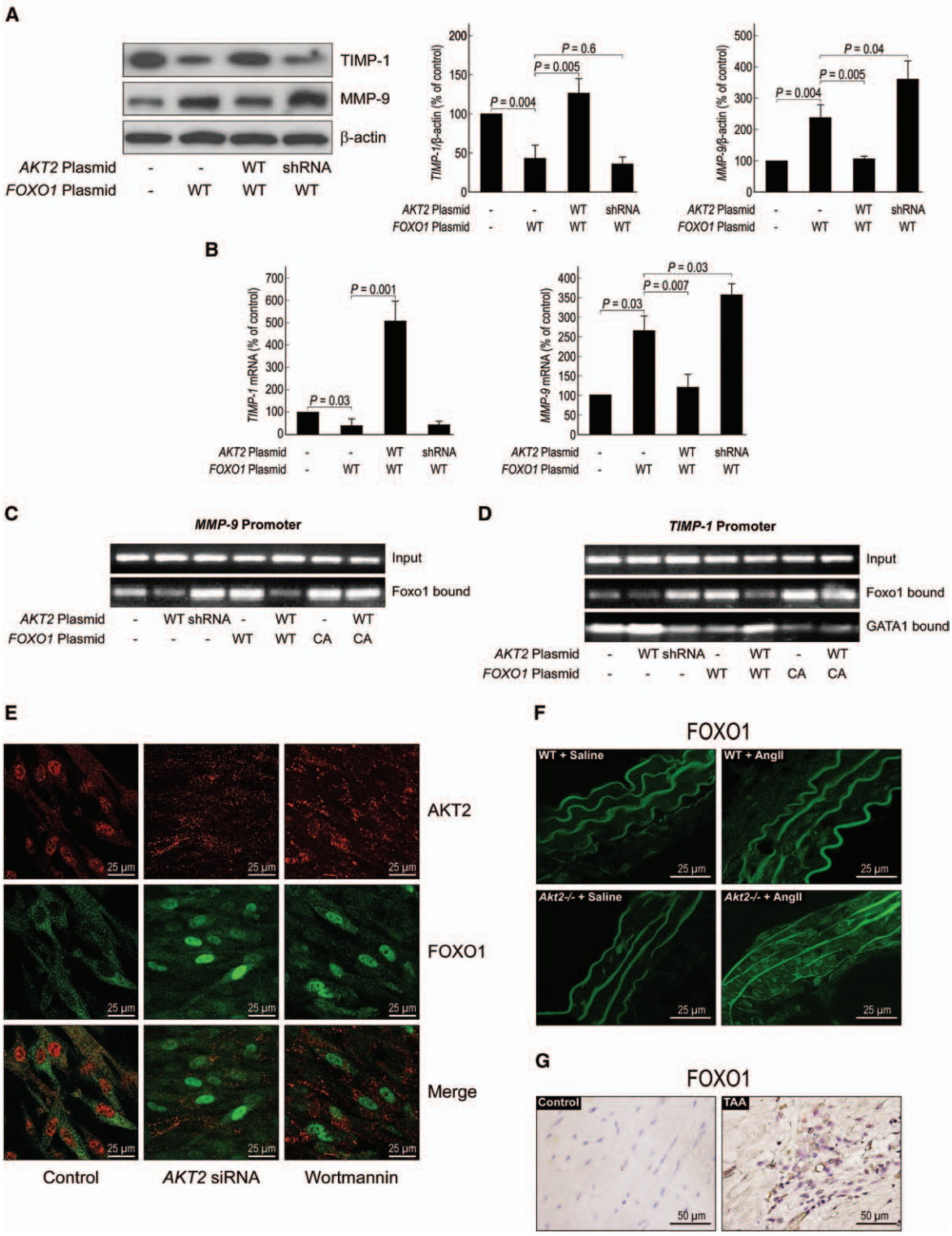

Figure 8. Inhibition of forkhead box protein O1 (FOXO1)–mediated matrix metalloproteinase (MMP)-9 expression by AKT2. Vascular smooth muscle cells were transfected with wild-type (WT)-*FOXO1* in the presence of WT-*AKT2* and *AKT2* short hairpin RNA (shRNA). **A**, MMP-9 and tissue inhibitor of metalloproteinase (TIMP)-1 protein levels were examined by Western blot. Representative blots from 3 independent experiments are shown. Quantification of the mean intensities of TIMP-1 and MMP-9 bands (normalized with those of β-actin) is shown. **B**, *MMP-9* and *TIMP-1* mRNA levels were examined by reverse transcription and quantitative real-time polymerase chain reaction and normalized with those of β-actin mRNA. The relative levels of mRNA are expressed as the percentage of the control. Data represent the mean±SD (n=3). **C**, FOXO1 binding to the *MMP-9* promoter was examined by chromatin immunoprecipitation (ChIP) analysis. **D**, FOXO1 and GATA1 binding to the *TIMP-1* promoter was examined by ChIP analysis. Representative blots from 2 independent experiments are shown. **E**, Immunostaining showed increased FOXO1 nuclear translocation in smooth muscle cells transfected with *Akt2* small interfering RNA (siRNA) or treated with Wortmannin. Immunostaining showed increased FOXO1 expression and nuclear localization in (**F**) aortas of angiotensin II (AngII)-infused *Akt2*$^{-/-}$ mice and (**G**) degenerative aortic media in human thoracic aortic aneurysm (TAA) tissue. CA indicates constitutively active.

SMC survival. AKT has well-established roles in promoting cell survival[6,21] by directly inhibiting apoptosis signal-regulating kinase 1,[22] p53,[22] and proapoptotic Bcl-2 protein BAD[23]—all key molecules in the apoptosis pathway. SMC apoptosis has been reported in human aortic aneurysms,[2,24] and it may play a critical role in SMC depletion and aortic damage during AAD formation. It is noteworthy that we observed a significant increase in the number of TUNEL-positive cells in the lesion regions of AngII-infused *Akt2*$^{-/-}$ mice, with more in dissected areas and fewer in areas with significant SMC loss. A high number of TUNEL-positive cells was also observed in human AAD tissues, even in those with significant SMC loss. In human abdominal aortic aneurysm with significant aortic SMC loss, the reported rate of apoptosis ranges from 10%[24] to 30%.[2] Interestingly, in our study, mice with a significant number of TUNEL-positive cells were alive at the end of the experiment (ie, 28 days after initiating AngII infusion; all ruptures occurred within 10 days of AngII infusion), indicating that profound tissue repair and fibrotic remodeling occurred in the aortic wall that strengthened the aortic wall structure and prevented rupture. Although it is unclear how rapidly TUNEL-positive cells in our study died, our evidence suggests that there was enough time for aortic repair and fibrotic remodeling to take place before rupture.

In mice challenged with AngII, we observed inflammatory cell infiltration in the aortic wall, which was significantly higher in the aortas of *Akt2*$^{-/-}$ mice than in WT mice, especially in dissected aortas. In AngII-infused *Akt2*$^{-/-}$ mice, most macrophages were observed in the adventitial layer. The complicated role of AKT in inflammation is not completely understood; although AKT has been shown to promote inflammation,[25] several studies have also shown that AKT activation can inhibit inflammation.[26–31] Given that AngII is known to induce inflammation,[32] the significant inflammatory cell infiltration observed in AngII-infused *Akt2*$^{-/-}$ mice may result from the insufficient inhibition of AngII-induced inflammation by AKT2. Another possibility is that the increased inflammatory cell infiltration in these mice represents a response to SMC apoptosis and aortic injury. The significant production of MMP-9 in macrophages suggests that these cells may contribute to aortic destruction.[32–34] Thus, when AngII-induced inflammation and aortic injury are not sufficiently counterbalanced, this may lead to inflammatory cell infiltration that causes further damage to the aortic wall.

MMPs are key destructive factors in the development of AAD.[35,36] MMP activity can be inhibited by TIMPs, and thus signaling pathways that regulate the balance between MMP and TIMP activities are critical in controlling tissue destruction. AKT has been shown to stimulate TIMP-1 expression in erythroid cells.[20] However, the AKT pathway has been shown to have complex effects on MMP regulation. Although AKT has been shown to promote MMP production in tumor invasion and metastasis,[37–39] recent studies have shown that the AKT pathway inhibits MMP expression. It has been suggested that PI3Kγ, a molecule upstream of AKT, inhibits the expression and activity of several MMPs induced by biomechanical stress.[40] In addition, the inhibition of the AKT pathway with rapamycin drastically enhanced the lipopolysaccharide-induced upregulation of MMP-9 in macrophages,[41] suggesting that the AKT pathway may negatively regulate MMP-9 expression. Here, we showed that AKT2 inhibited MMP-9 expression and stimulated TIMP-1 expression in cultured VSMCs. In AngII-infused *Akt2*$^{-/-}$ mice, MMP-9 expression was significantly elevated in aortic SMCs. In addition, the induction of TIMP-1 in response to increased MMPs was significantly lower and the MMP-9/TIMP-1 ratio was significantly higher in AngII-infused *Akt2*$^{-/-}$ mice than in WT mice. Thus, our findings suggest that the AKT2-induced inhibition of MMP-9 and stimulation of TIMP-1 in VSMCs may contribute to the protective effects of AKT2 on the aorta.

In our study, we also found that AKT2 stimulated TIMP-1 and inhibited MMP-9 expression through the inhibition of FOXO1. We showed that FOXO1 upregulated MMP-9 and downregulated TIMP-1 expression, which was reversed by the overexpression of AKT2. Consistent with these observations, a recent study showed that FOXO3 induces the expression of MMP-9 and MMP-13 in cancer cells and promotes tumor metastasis.[42] FOXO3a has also been shown to increase MMP-3 expression and activity and decrease TIMP-1 expression in the vascular wall.[43] In several regions of the *TIMP-1* promoter, we identified FOXO1 binding sites in close proximity to binding sites of GATA1. Given our finding that FOXO1 can bind to the *TIMP-1* promoter and prevent the DNA binding of GATA1, it is conceivable that FOXO1 binding to the *TIMP-1* promoter may prevent GATA1 DNA binding and suppress *TIMP-1* transcription. AKT has previously been shown to induce TIMP-1 expression by directly phosphorylating and activating GATA1.[20] Thus, in addition to activating GATA1, AKT2 may also promote TIMP-1 expression by preventing FOXO1 from inhibiting the DNA binding of GATA1 to the *TIMP-1* promoter. Our finding that AKT2 regulates MMP-9 and TIMP-1 expression by inhibiting FOXO1 represents a novel mechanism for the control of MMP and TIMP production (Online Figure IV).

Other mechanisms may underlie the protective effects of AKT2. For example, AKT has been shown to inhibit RhoA, a downstream target of the AngII-signaling pathway.[29] AKT also can inhibit transforming growth factor-β signaling,[44,45] a critical player in aortic destruction and aneurysm formation. In addition, AKT plays a significant role in VSMC proliferation,[46] migration,[46] differentiation,[47,48] ECM protein production, and aortic repair (our unpublished observations). AKT2 also plays critical roles in glucose[49,50] and lipid[51,52] homeostasis. As a result, even though we used young mice (8 weeks old) to avoid profound metabolic disturbance, the metabolic stress from *Akt2* deficiency may also partially contribute to aortic destruction in these mice. Further studies are needed to explore this possibility. Finally, AKT may play an important role in aortic wall development; impaired formation of aortic ECM could cause developmental abnormalities that predispose *Akt2*-deficient mice to AAD formation after the infusion of AngII.

The AKT kinase family comprises 3 highly homologous isoforms that have specific functions. AKT1 promotes cell survival,[53] and AKT2 regulates glucose[49,50] and lipid[51,52] homeostasis. AKT3 has recently been shown to reduce lipoprotein uptake in macrophages, preventing foam cell formation that

leads to atherosclerosis development.[54] However, evidence suggests that AKT isoforms share many of these functions. For example, AKT2 also plays a critical role in promoting cell survival.[55–57] We have also observed the regulation of MMP-9 and TIMP-1 by AKT1 (data not shown), although AKT1 showed stronger inhibition of MMP-9, and AKT2 showed stronger induction of TIMP-1. Thus, AKT isoforms may act cooperatively to balance TIMPs and MMPs.

We observed significantly reduced levels of active AKT and AKT2 in human TAA and TAD tissues than in control aortas. Interestingly, AKT expression within the diseased aorta exhibited marked heterogeneity; although AKT expression was downregulated in degenerative areas, it was abundantly expressed in preserved areas and in hyperplastic areas. This pattern of variation in AKT expression is consistent with the heterogeneic nature of aortic aneurysm pathology; different areas of the aortic wall exhibit different stages of disease progression, even within a single aneurysm. Importantly, regardless of overall AKT expression, phospho-AKT levels were significantly lower in the aortic media of patients with AAD than in those of age-matched controls, indicating impaired AKT signaling in diseased aortas. The low levels of active AKT observed in diseased aortas may have resulted from reduced cell numbers or from decreased AKT expression and impaired AKT activation in the remaining cells.

In this study, our age-matched control subjects had a mean age of 61 years; many of these subjects had hypertension, dyslipidemia, and diabetes mellitus. Considerable variation in active AKT levels was observed among control tissues. Interestingly, high levels of active AKT were often observed in aortic tissues from control subjects with diabetes mellitus. Similar to our patients, control subjects with diabetes mellitus were presumably exposed to inflammatory and metabolic stress generated from their comorbid condition. The activation of AKT in the aorta of these individuals may provide protection against such biological insults and counterbalance the stress/destructive factors and pathways.

Compromised AKT signaling has been reported in the thoracic aorta of patients with Marfan syndrome.[58] Given the importance of the AKT signaling pathway in protecting the aorta, the downregulation of this pathway may be partially responsible for the formation and progression of thoracic AAD in Marfan syndrome patients. Further studies are necessary to elucidate the causes of AKT downregulation in the aorta. It is well established that inflammation[12] and metabolic stress[13] can impair AKT signaling. The aorta, especially in aged individuals with atherosclerosis, is constantly exposed to inflammatory factors and metabolic stress that may affect the medial layer of the aorta and impair AKT signaling.

Conclusion

Our findings suggest that AKT2 may have a protective role against AAD in humans. Although these findings require further validation, the possibility remains that the preservation of AKT2 signaling may be an effective strategy for preventing the formation of AAD.

Acknowledgments

We gratefully acknowledge Sue Zhang of the Texas Heart Institute at St. Luke's Episcopal Hospital for critical discussion of the article; Darren Woodside and Deenadayalan Bakthavatsalam of the Texas Heart Institute at St. Luke's Episcopal Hospital for their expert advice regarding use of the confocal microscope; Scott A. Weldon of Baylor College of Medicine for assistance with illustrations; and Nicole Stancel of the Texas Heart Institute at St. Luke's Episcopal Hospital for providing editorial support.

Sources of Funding

This study was supported by National Institutes of Health (NIH) R01HL085341 (to S.A. LeMaire), NIH K08 HL080085 (to S.A. LeMaire) and the Thoracic Surgery Foundation for Education and Research (to S.A. LeMaire). The Thoracic Aortic Disease Tissue Bank at Baylor College of Medicine was supported, in part, through the Tissue Banking Core of the Specialized Center of Clinically Oriented Research in Thoracic Aortic Aneurysms and Dissections (NIH P50 HL083794).

Disclosures

None.

References

1. Kochanek KD, Kirmeyer SE, Martin JA, Strobino DM, Guyer B. Annual summary of vital statistics: 2009. *Pediatrics*. 2012;129:338–348.
2. López-Candales A, Holmes DR, Liao S, Scott MJ, Wickline SA, Thompson RW. Decreased vascular smooth muscle cell density in medial degeneration of human abdominal aortic aneurysms. *Am J Pathol*. 1997;150:993–1007.
3. Schlatmann TJ, Becker AE. Pathogenesis of dissecting aneurysm of aorta. Comparative histopathologic study of significance of medial changes. *Am J Cardiol*. 1977;39:21–26.
4. Manning BD, Cantley LC. AKT/PKB signaling: navigating downstream. *Cell*. 2007;129:1261–1274.
5. Shiojima I, Walsh K. Role of Akt signaling in vascular homeostasis and angiogenesis. *Circ Res*. 2002;90:1243–1250.
6. Fujio Y, Nguyen T, Wencker D, Kitsis RN, Walsh K. Akt promotes survival of cardiomyocytes in vitro and protects against ischemia-reperfusion injury in mouse heart. *Circulation*. 2000;101:660–667.
7. Matsui T, Tao J, del Monte F, Lee KH, Li L, Picard M, Force TL, Franke TF, Hajjar RJ, Rosenzweig A. Akt activation preserves cardiac function and prevents injury after transient cardiac ischemia in vivo. *Circulation*. 2001;104:330–335.
8. Condorelli G, Drusco A, Stassi G, Bellacosa A, Roncarati R, Iaccarino G, Russo MA, Gu Y, Dalton N, Chung C, Latronico MV, Napoli C, Sadoshima J, Croce CM, Ross J Jr. Akt induces enhanced myocardial contractility and cell size in vivo in transgenic mice. *Proc Natl Acad Sci USA*. 2002;99:12333–12338.
9. Matsui T, Li L, Wu JC, Cook SA, Nagoshi T, Picard MH, Liao R, Rosenzweig A. Phenotypic spectrum caused by transgenic overexpression of activated Akt in the heart. *J Biol Chem*. 2002;277:22896–22901.
10. Nagoshi T, Matsui T, Aoyama T, Leri A, Anversa P, Li L, Ogawa W, del Monte F, Gwathmey JK, Grazette L, Hemmings BA, Hemmings B, Kass DA, Champion HC, Rosenzweig A. PI3K rescues the detrimental effects of chronic Akt activation in the heart during ischemia/reperfusion injury. *J Clin Invest*. 2005;115:2128–2138.
11. Luo Z, Fujio Y, Kureishi Y, Rudic RD, Daumerie G, Fulton D, Sessa WC, Walsh K. Acute modulation of endothelial Akt/PKB activity alters nitric oxide-dependent vasomotor activity in vivo. *J Clin Invest*. 2000;106:493–499.
12. Shen YH, Zhang L, Gan Y, Wang X, Wang J, LeMaire SA, Coselli JS, Wang XL. Up-regulation of PTEN (phosphatase and tensin homolog deleted on chromosome ten) mediates p38 MAPK stress signal-induced inhibition of insulin signaling. A cross-talk between stress signaling and insulin signaling in resistin-treated human endothelial cells. *J Biol Chem*. 2006;281:7727–7736.
13. Wang XL, Zhang L, Youker K, Zhang MX, Wang J, LeMaire SA, Coselli JS, Shen YH. Free fatty acids inhibit insulin signaling-stimulated

endothelial nitric oxide synthase activation through upregulating PTEN or inhibiting Akt kinase. *Diabetes*. 2006;55:2301–2310.
14. Shigematsu K, Koyama H, Olson NE, Cho A, Reidy MA. Phosphatidylinositol 3-kinase signaling is important for smooth muscle cell replication after arterial injury. *Arterioscler Thromb Vasc Biol*. 2000;20:2373–2378.
15. Auge N, Garcia V, Maupas-Schwalm F, Levade T, Salvayre R, Negre-Salvayre A. Oxidized LDL-induced smooth muscle cell proliferation involves the EGF receptor/PI-3 kinase/Akt and the sphingolipid signaling pathways. *Arterioscler Thromb Vasc Biol*. 2002;22:1990–1995.
16. Stabile E, Zhou YF, Saji M, Castagna M, Shou M, Kinnaird TD, Baffour R, Ringel MD, Epstein SE, Fuchs S. Akt controls vascular smooth muscle cell proliferation in vitro and in vivo by delaying G1/S exit. *Circ Res*. 2003;93:1059–1065.
17. Yao JS, Chen Y, Zhai W, Xu K, Young WL, Yang GY. Minocycline exerts multiple inhibitory effects on vascular endothelial growth factor-induced smooth muscle cell migration: the role of ERK1/2, PI3K, and matrix metalloproteinases. *Circ Res*. 2004;95:364–371.
18. Calabro P, Samudio I, Willerson JT, Yeh ET. Resistin promotes smooth muscle cell proliferation through activation of extracellular signal-regulated kinase 1/2 and phosphatidylinositol 3-kinase pathways. *Circulation*. 2004;110:3335–3340.
19. Daugherty A, Manning MW, Cassis LA. Antagonism of AT2 receptors augments angiotensin II-induced abdominal aortic aneurysms and atherosclerosis. *Br J Pharmacol*. 2001;134:865–870.
20. Kadri Z, Maouche-Chretien L, Rooke HM, Orkin SH, Romeo PH, Mayeux P, Leboulch P, Chretien S. Phosphatidylinositol 3-kinase/Akt induced by erythropoietin renders the erythroid differentiation factor GATA-1 competent for TIMP-1 gene transactivation. *Mol Cell Biol*. 2005;25:7412–7422.
21. Amaravadi R, Thompson CB. The survival kinases Akt and Pim as potential pharmacological targets. *J Clin Invest*. 2005;115:2618–2624.
22. Kim AH, Khursigara G, Sun X, Franke TF, Chao MV. Akt phosphorylates and negatively regulates apoptosis signal-regulating kinase 1. *Mol Cell Biol*. 2001;21:893–901.
23. Datta SR, Dudek H, Tao X, Masters S, Fu H, Gotoh Y, Greenberg ME. Akt phosphorylation of BAD couples survival signals to the cell-intrinsic death machinery. *Cell*. 1997;91:231–241.
24. Henderson EL, Geng YJ, Sukhova GK, Whittemore AD, Knox J, Libby P. Death of smooth muscle cells and expression of mediators of apoptosis by T lymphocytes in human abdominal aortic aneurysms. *Circulation*. 1999;99:96–104.
25. Calamito M, Juntilla MM, Thomas M, Northrup DL, Rathmell J, Birnbaum MJ, Koretzky G, Allman D. Akt1 and Akt2 promote peripheral B-cell maturation and survival. *Blood*. 2010;115:4043–4050.
26. Guha M, Mackman N. The phosphatidylinositol 3-kinase-Akt pathway limits lipopolysaccharide activation of signaling pathways and expression of inflammatory mediators in human monocytic cells. *J Biol Chem*. 2002;277:32124–32132.
27. Schabbauer G, Tencati M, Pedersen B, Pawlinski R, Mackman N. PI3K-Akt pathway suppresses coagulation and inflammation in endotoxemic mice. *Arterioscler Thromb Vasc Biol*. 2004;24:1963–1969.
28. Yin W, Signore AP, Iwai M, Cao G, Gao Y, Johnnides MJ, Hickey RW, Chen J. Preconditioning suppresses inflammation in neonatal hypoxic ischemia via Akt activation. *Stroke*. 2007;38:1017–1024.
29. Zhang WJ, Wei H, Hagen T, Frei B. Alpha-lipoic acid attenuates LPS-induced inflammatory responses by activating the phosphoinositide 3-kinase/Akt signaling pathway. *Proc Natl Acad Sci USA*. 2007;104:4077–4082.
30. Kidd LB, Schabbauer GA, Luyendyk JP, Holscher TD, Tilley RE, Tencati M, Mackman N. Insulin activation of the phosphatidylinositol 3-kinase/protein kinase B (Akt) pathway reduces lipopolysaccharide-induced inflammation in mice. *J Pharmacol Exp Ther*. 2008;326:348–353.
31. Carpintero R, Brandt KJ, Gruaz L, Molnarfi N, Lalive PH, Burger D. Glatiramer acetate triggers PI3Kδ/Akt and MEK/ERK pathways to induce IL-1 receptor antagonist in human monocytes. *Proc Natl Acad Sci USA*. 2010;107:17692–17697.
32. Tieu BC, Lee C, Sun H, Lejeune W, Recinos A III, Ju X, Spratt H, Guo DC, Milewicz D, Tilton RG, Brasier AR. An adventitial IL-6/MCP1 amplification loop accelerates macrophage-mediated vascular inflammation leading to aortic dissection in mice. *J Clin Invest*. 2009;119:3637–3651.
33. Sun J, Sukhova GK, Yang M, Wolters PJ, MacFarlane LA, Libby P, Sun C, Zhang Y, Liu J, Ennis TL, Knispel R, Xiong W, Thompson RW, Baxter BT, Shi GP. Mast cells modulate the pathogenesis of elastase-induced abdominal aortic aneurysms in mice. *J Clin Invest*. 2007;117:3359–3368.
34. Xiong W, MacTaggart J, Knispel R, Worth J, Persidsky Y, Baxter BT. Blocking TNF-alpha attenuates aneurysm formation in a murine model. *J Immunol*. 2009;183:2741–2746.
35. Segura AM, Luna RE, Horiba K, Stetler-Stevenson WG, McAllister HA Jr, Willerson JT, Ferrans VJ. Immunohistochemistry of matrix metalloproteinases and their inhibitors in thoracic aortic aneurysms and aortic valves of patients with Marfan's syndrome. *Circulation*. 1998;98:II331–II337; discussion II337.
36. Zhang X, Shen YH, LeMaire SA. Thoracic aortic dissection: are matrix metalloproteinases involved? *Vascular*. 2009;17:147–157.
37. Cheng JC, Chou CH, Kuo ML, Hsieh CY. Radiation-enhanced hepatocellular carcinoma cell invasion with MMP-9 expression through PI3K/Akt/NF-kappaB signal transduction pathway. *Oncogene*. 2006;25:7009–7018.
38. Zhang D, Bar-Eli M, Meloche S, Brodt P. Dual regulation of MMP-2 expression by the type 1 insulin-like growth factor receptor: the phosphatidylinositol 3-kinase/Akt and Raf/ERK pathways transmit opposing signals. *J Biol Chem*. 2004;279:19683–19690.
39. Zhang D, Brodt P. Type 1 insulin-like growth factor regulates MT1-MMP synthesis and tumor invasion via PI 3-kinase/Akt signaling. *Oncogene*. 2003;22:974–982.
40. Guo D, Kassiri Z, Basu R, Chow FL, Kandalam V, Damilano F, Liang W, Izumo S, Hirsch E, Penninger JM, Backx PH, Oudit GY. Loss of pi3kγ enhances cAMP-dependent MMP remodeling of the myocardial N-cadherin adhesion complexes and extracellular matrix in response to early biomechanical stress. *Circ Res*. 2010;107:1275-1289.
41. Mendes Sdos S, Candi A, Vansteenbrugge M, Pignon MR, Bult H, Boudjeltia KZ, Munaut C, Raes M. Microarray analyses of the effects of NF-kappaB or PI3K pathway inhibitors on the LPS-induced gene expression profile in RAW264.7 cells: synergistic effects of rapamycin on LPS-induced MMP9-overexpression. *Cell Signal*. 2009;21:1109–1122.
42. Storz P, Döppler H, Copland JA, Simpson KJ, Toker A. FOXO3a promotes tumor cell invasion through the induction of matrix metalloproteinases. *Mol Cell Biol*. 2009;29:4906–4917.
43. Lee HY, You HJ, Won JY, Youn SW, Cho HJ, Park KW, Park WY, Seo JS, Park YB, Walsh K, Oh BH, Kim HS. Forkhead factor, FOXO3a, induces apoptosis of endothelial cells through activation of matrix metalloproteinases. *Arterioscler Thromb Vasc Biol*. 2008;28:302–308.
44. Conery AR, Cao Y, Thompson EA, Townsend CM Jr, Ko TC, Luo K. Akt interacts directly with Smad3 to regulate the sensitivity to TGF-beta induced apoptosis. *Nat Cell Biol*. 2004;6:366–372.
45. Remy I, Montmarquette A, Michnick SW. PKB/Akt modulates TGF-beta signalling through a direct interaction with Smad3. *Nat Cell Biol*. 2004;6:358–365.
46. Poon M, Marx SO, Gallo R, Badimon JJ, Taubman MB, Marks AR. Rapamycin inhibits vascular smooth muscle cell migration. *J Clin Invest*. 1996;98:2277–2283.
47. Martin KA, Merenick BL, Ding M, Fetalvero KM, Rzucidlo EM, Kozul CD, Brown DJ, Chiu HY, Shyu M, Drapeau BL, Wagner RJ, Powell RJ. Rapamycin promotes vascular smooth muscle cell differentiation through insulin receptor substrate-1/phosphatidylinositol 3-kinase/Akt2 feedback signaling. *J Biol Chem*. 2007;282:36112–36120.
48. Ackah E, Yu J, Zoellner S, Iwakiri Y, Skurk C, Shibata R, Ouchi N, Easton RM, Galasso G, Birnbaum MJ, Walsh K, Sessa WC. Akt1/protein kinase Bα is critical for ischemic and VEGF-mediated angiogenesis. *J Clin Invest*. 2005;115:2119–2127.
49. Cho H, Mu J, Kim JK, Thorvaldsen JL, Chu Q, Crenshaw EB III, Kaestner KH, Bartolomei MS, Shulman GI, Birnbaum MJ. Insulin resistance and a diabetes mellitus-like syndrome in mice lacking the protein kinase Akt2 (PKB beta). *Science*. 2001;292:1728–1731.
50. Garofalo RS, Orena SJ, Rafidi K, Torchia AJ, Stock JL, Hildebrandt AL, Coskran T, Black SC, Brees DJ, Wicks JR, McNeish JD, Coleman KG. Severe diabetes, age-dependent loss of adipose tissue, and mild growth deficiency in mice lacking Akt2/PKB beta. *J Clin Invest*. 2003;112:197–208.
51. Leavens KF, Easton RM, Shulman GI, Previs SF, Birnbaum MJ. Akt2 is required for hepatic lipid accumulation in models of insulin resistance. *Cell Metab*. 2009;10:405–418.
52. Wan M, Leavens KF, Saleh D, Easton RM, Guertin DA, Peterson TR, Kaestner KH, Sabatini DM, Birnbaum MJ. Postprandial hepatic

lipid metabolism requires signaling through Akt2 independent of the transcription factors FoxA2, FoxO1, and SREBP1c. *Cell Metab*. 2011;14:516–527.
53. Chen WS, Xu PZ, Gottlob K, Chen ML, Sokol K, Shiyanova T, Roninson I, Weng W, Suzuki R, Tobe K, Kadowaki T, Hay N. Growth retardation and increased apoptosis in mice with homozygous disruption of the Akt1 gene. *Genes Dev*. 2001;15:2203–2208.
54. Ding L, Biswas S, Morton RE, Smith JD, Hay N, Byzova TV, Febbraio M, Podrez EA. Akt3 deficiency in macrophages promotes foam cell formation and atherosclerosis in mice. *Cell Metab*. 2012;15:861–872.
55. Bacus SS, Altomare DA, Lyass L, Chin DM, Farrell MP, Gurova K, Gudkov A, Testa JR. AKT2 is frequently upregulated in HER-2/neu-positive breast cancers and may contribute to tumor aggressiveness by enhancing cell survival. *Oncogene*. 2002;21:3532–3540.
56. Fujio Y, Mitsuuchi Y, Testa JR, Walsh K. Activation of Akt2 inhibits anoikis and apoptosis induced by myogenic differentiation. *Cell Death Differ*. 2001;8:1207–1212.
57. Kim MA, Kim HJ, Jee HJ, Kim AJ, Bae YS, Bae SS, Yun J. Akt2, but not Akt1, is required for cell survival by inhibiting activation of JNK and p38 after UV irradiation. *Oncogene*. 2009;28:1241–1247.
58. Chung AW, Au Yeung K, Cortes SF, Sandor GG, Judge DP, Dietz HC, van Breemen C. Endothelial dysfunction and compromised eNOS/Akt signaling in the thoracic aorta during the progression of Marfan syndrome. *Br J Pharmacol*. 2007;150:1075–1083.

Novelty and Significance

What Is Known?

- Open and endovascular surgical repair of aortic aneurysm and dissection (AAD) are accompanied by high perioperative morbidity and mortality, and medical therapy to prevent the formation and progression of AAD is lacking.
- AAD are caused by the progressive degeneration of the aortic media, characterized by the depletion of smooth muscle cells and the destruction of extracellular matrix.
- Although the overproduction of destructive factors promotes tissue damage and AAD progression, the role of pathways that protect against the development of AAD is unknown.

What New Information Does This Article Contribute?

- Levels of AKT2 protein and phospho-AKT are significantly downregulated in human thoracic AAD tissues.
- A causal relationship between *Akt2* deficiency and AAD is supported by our findings that the aortas of *Akt2*-deficient mice challenged with angiotensin II (but not the aortas of wild-type mice challenged with angiotensin II) developed aneurysm, dissection, and rupture and showed evidence of profound tissue destruction and apoptotic cell death.
- The mechanism of AKT2 protection against AAD involves the inhibition of matrix metalloproteinase-9 and the stimulation of tissue inhibitor of metalloproteinase-1 through the inhibition of the transcription factor forkhead box protein O1.

AAD are characterized by degeneration of the aortic media. The role of the pathways that protect against AAD is unknown. We examined the role of AKT2 in AAD formation. We found that protein levels of AKT2 and phospho-AKT were significantly reduced in human thoracic AAD tissues, especially within the degenerative medial layer. Our studies in *Akt2*-deficient mice showed that these mice have abnormal elastic fibers and reduced medial thickness in the aortic wall. When challenged with AngII, *Akt2*-deficient mice developed aortic aneurysm, dissection, and rupture. Aortas from AngII-infused *Akt2*-deficient mice displayed profound tissue destruction, apoptotic cell death, and inflammatory cell infiltration—changes that were not observed in aortas from AngII-infused wild-type mice. Additional findings in *Akt2*-deficient mice and human aortic vascular smooth muscle cells indicated that the protective mechanism of AKT2 involves the regulation of matrix metalloproteinase-9 and tissue inhibitor of metalloproteinase-1 expression. The results of these studies showing that impaired AKT2 signaling may contribute to AAD formation may lead to the development of a new therapeutic target for the treatment of AAD.

Supplemental Material

Detailed Methods

Patient Enrollment and Tissue Collection

Patients with aortitis, connective tissue disorders, or ruptured aneurysm were excluded. During surgery, aortic tissues were collected from the largest portion of the aneurysm (portions of this area of the aorta are routinely excised and discarded during repair). In patients with TAD, samples were taken from the outer wall of the false lumen. Control descending thoracic aortic tissue was collected from 12 age-matched organ donors (age, 61.3±7.1 years) without aortic aneurysm, dissection, coarctation, or previous aortic repair (The International Institute for the Advancement of Medicine, Jessup, PA). Periaortic fat and intraluminal thrombus were trimmed away, and the samples were rinsed with saline. Samples were snap frozen and stored at –80°C for protein analysis or fixed in 10% formaldehyde and embedded for histologic and immunohistochemical analysis.

Animal Studies

Eight-week-old WT and *Akt2-/-* male mice were infused with either saline or 1,000 ng/min/kg angiotensin II (AngII; Sigma-Aldrich, St. Louis, MO) for 28 days[2] by using osmotic minipumps (Model 2004; ALZA Scientific Products, Mountain View, CA). Systolic blood pressure was measured weekly in conscious mice by using the noninvasive tail-cuff Visitech BP-2000 system (Visitech Systems, Apex, NC). At the end of the 28-day infusion, mice were euthanized, and their aortas were irrigated with phosphate-buffered saline (PBS). Aortas were either fixed in 10% formaldehyde for diameter measurement, histologic analysis, and immunohistochemical analysis or fixed in OCT for immunofluorescence staining and *in situ* zymography staining.

Characterization of Aortic Gross Pathology in Mice

The severity of each aneurysm and dissection was assessed on the basis of the gross appearance of the aorta according to the classification of Daugherty and colleagues,[3] with slight modifications: Type I, aorta with dilated lumen without thrombus; Type II, aorta with tissue destruction that contains thrombus; Type III, aorta with a pronounced bulbous form that contains thrombus; Type IV, aorta with multiple aneurysms containing thrombus; and Type V, ruptured aorta. Aneurysmal tissue was classified independently by 2 observers blinded to the animal study. There was complete concordance between the observers.

Elastic Fiber Staining and Grading

Paraffin-embedded aortic sections were stained with Verhoeff–van Gieson elastin staining by using the Elastic Stain kit (Sigma-Aldrich) according to the manufacturer's instructions. Aortic sections were examined by 4 independent observers who were blinded to the animal group allocation. Elastic fiber fragmentation was scored (Grade 0 = none; Grade 1 = minimal; Grade 2 = moderate; Grade 3 = severe). The thickness of the aortic medial layer was measured at 3 randomly selected sites to calculate the average aortic medial thickness.

Immunohistochemistry and Immunofluorescence Staining

For immunohistochemical analysis, formalin-fixed, paraffin-embedded aortic sections were deparaffinized and rehydrated before antigen retrieval in citrate buffer (pH = 6.0-6.2) or Tris-EDTA buffer (pH = 9.0). Endogenous peroxidase activity was quenched by incubating the slides with 3% hydrogen peroxide, and nonspecific staining was reduced by blocking with 5% normal blocking serum. The sections were incubated with primary antibodies at 4°C overnight and then with secondary antibody, before staining with 3,3-diaminobenzidine by using the VECTASTAIN

ABC kit (Vector Laboratories, Inc.; Burlingame, CA). Nuclei were counterstained with hematoxylin. Slides incubated with IgG alone were used as negative controls.

For immunofluorescence staining, frozen sections were fixed with Cytofix (BD Biosciences**,** San Jose, CA), and cells were permeabilized with Perm/Wash (BD Biosciences). Nonspecific staining was reduced by blocking with 5% normal blocking serum. Sections were stained with primary antibodies at room temperature for 2 hours or at 4°C overnight and then stained with secondary antibodies conjugated to an Alexa Fluor dye (ie, Alexa Fluor 568 or 488; Invitrogen, Carlsbad, CA). Nuclei were counterstained with 4',6-Diamidino-2-phenylindole dihydrochloride (DAPI). Slides incubated with secondary antibodies were used as negative controls. For immunohistochemistry and immunofluorescence studies, antibodies against SM22a (Abcam, Cambridge, MA), CD68, CD3, MMP-9, MMP-2, TIMP-1 (Santa Cruz Biotechnology, Santa Cruz, CA), FOXO-1, AIF, and cleaved caspase-3 (Cell Signaling Technology, Danvers, MA) were used.

Sections were examined by using an Olympus DP70 fluorescence microscope (Olympus, Tokyo, Japan) or Leica SP5 confocal microscope (Leica Microsystems Inc., Buffalo Grove, IL). Images from 5-8 randomly selected visual fields (excluding the thrombosed false lumen) (magnification, 400×) per aortic section were captured, and the positive signal (positive cells or positive-staining area, without selecting autofluorescent elastic fibers) and the evaluated area were measured by using Image-Pro Plus V7.0 software (Media Cybernetics, Inc., Bethesda, MD). The positive signals were normalized to the evaluated aortic area, and the mean positive signals were calculated and compared between groups.

In Situ Zymography

MMP activity in the aortic wall was determined by using gelatin conjugated with quenched fluorescein (DQ gelatin; Invitrogen) as a substrate, according to the manufacturer's instructions. Briefly, frozen aortic sections were incubated with 0.1 mg/mL DQ gelatin in 1% low-melting agarose at 37°C for 48 hours. Fluorescence was examined by using fluorescence microscopy. Zymographic images were acquired by using identical setting and exposure times.

Analysis of Apoptosis With the TUNEL Assay

Apoptosis was studied by using the terminal deoxynucleotidyl transferase-mediated dUTP-biotin nick end labeling (TUNEL) assay. Apoptotic cells were detected by using an in situ cell death detection kit (Roche Applied Science, Indianapolis, IA) as described previously.[4] Briefly, frozen sections of aorta were fixed with 4% paraformaldehyde in PBS for 10 minutes and permeabilized with 0.2% Triton X-100 for 5 minutes. The fixed cells were incubated for 1 hour at 37°C with TUNEL reaction mixture containing terminal deoxynucleotidyl transferase. Nuclei were counterstained with DAPI (0.1 g/mL) after TUNEL staining. Terminal deoxynucleotidyl transferase–free labeling mixture was used in negative control reactions. The capture of images and the quantification of positive cells were performed as described above.

Cell Culture and Transfection

Human aortic VSMCs (Cell Applications, San Diego, CA) were cultured in smooth muscle media (Invitrogen) with 10% fetal bovine serum. VSMCs were transfected with plasmid DNA, siRNA, or shRNA by using Lipofectamine (Invitrogen) according to the manufacturer's instructions. Transfected cells were then treated with factors such as transforming growth factor-β (TGF-β). Transfection efficiency was confirmed by Western blot. Wild-type (WT)-*AKT1*, dominant negative (DN)-*AKT1*, WT-*FOXO1*, constitutively active (CA)-*FOXO1*, and DN-

FOXO1 plasmids from Addgene Inc. (Cambridge, MA) and WT-*AKT2* plasmid and *AKT2* shRNA from OriGene Technologies (Rockville, MD) were used in this study.

Western Blot Analysis

Treated cells were collected and lysed as previously described.[5] Protein samples (15 μg per lane) were subjected to sodium dodecyl sulfate polyacrylamide gel electrophoresis (SDS-PAGE) and were transferred to PVDF membranes. The membranes were blocked, incubated with primary antibody, washed, and incubated with secondary HRP-labeled antibody. Bands were visualized by enhanced chemiluminescence (Amersham Biosciences, Piscataway, NJ). Protein bands, including those for β-actin, were quantified by densitometry with the Quantity One imaging program (Bio-Rad, Hercules, CA). Protein levels were normalized to those of β-actin and expressed as the percentage of the no-treatment control. For Western blot analysis, primary antibodies against MMP-9 (Abcam), TIMP-1 (Santa Cruz Biotechnology), phospho-AKT (Ser 473), pan-AKT, AKT-1, AKT-2, FOXO-1 (Cell Signaling Technology) were used.

Quantitative Real-Time Polymerase Chain Reaction (qRT-PCR)

Total RNA from aortic tissue and treated cells was extracted with Trizol (Invitrogen) according to the manufacturer's protocol. The mRNAs were reverse-transcribed with the iScript cDNA synthesis kit (Bio-Rad). qRT-PCR was performed with the iCycler iQ Real Time PCR detection system (Bio-Rad). Primers were designed with Beacon Designer 2.0 software (Premier Biosoft International, Palo Alto, CA). We used the following primers: for mouse *Mmp-9*: forward 5'-CTCACTCACTGTGGTTGCTG-3'and reverse 5'-TGGTTATCCTTCCTGGATCA-3'; for mouse *Timp-1*: forward 5'-GGCATCCTCTTGTTGCTATCACTG-3' and reverse 5'-GTCATCTTGATCTCATAACGCTGG-3'; for human *MMP-9*: forward 5'-CCGGACCAAGGATACAGTTT-3' and reverse 5'- GCCATTCACGTCGTCCTTAT-3'; and for

human tissue inhibitor of metalloproteinase-1 (*TIMP-1*): forward 5'-AATTCCGACCTCGTCATCAG-3' and reverse 5'- TGCAGTTTCCAGCAATGAG-3'. mRNA levels were determined by normalizing the cycle threshold (Ct) of *MMP-9* or *TIMP-1* to the Ct of β-actin. The relative levels of mRNA were compared and expressed as the percentage of the no-treatment control.

Chromatin Immunoprecipitation (ChIP) Assay

The ChIP assay was performed by using a ChIP assay kit (Upstate Biotechnology, Inc., Lake Placid, NY) as described previously.[6] In brief, VSMCs transfected with plasmid or siRNA were first incubated with 1% formaldehyde at 37°C for 15 min to cross link DNA-protein complexes. Cells were then rinsed, harvested, and lysed. Cell lysates were sonicated and centrifuged to produce chromatin fragments of 300–1000 bp in length. The supernatants were precleared with a mixture of salmon sperm DNA/protein A/protein G, followed by immunoprecipitation with anti-FOXO1 antibody–protein A-agarose slurry or with IgG (negative control). The immunocomplex beads were then washed sequentially with low-salt wash buffer, high-salt wash buffer, LiCl wash buffer, and TE buffer. The immunocomplex was eluted with elution buffer (100 mM $NaHCO_3$, 1% SDS). The eluted immunocomplex and the inputs were incubated with 200 mM NaCl at 65°C overnight to reverse cross-linking, followed by incubation with proteinase K to digest the remaining proteins. DNA was recovered by phenol/chloroform/isoamyl alcohol extraction and used as a template for PCR. The PCR products were separated by electrophoresis on a 1.5% agarose gel. The primers used to detect FOXO binding site in the 5'-flanking region of the human *MMP-9* gene were as follows: forward primer 5'-CATTTCTGGTTGTCACAACT-3' and reverse primer 5'-TATCTATGTATGTATGTCAC-3'; The primers used to detect FOXO and GATA binding sites in the 5'-flanking region of the human *TIMP-1* gene were as follows:

forward primer 5'-GTTATTGGGCTATCATCCCT-3' and reverse primer 5'-GAGGATAGATCAATAATAAT -3'.

Supplemental References

1. Cho H, Mu J, Kim JK, Thorvaldsen JL, Chu Q, Crenshaw EB, 3rd, Kaestner KH, Bartolomei MS, Shulman GI, Birnbaum MJ. Insulin resistance and a diabetes mellitus-like syndrome in mice lacking the protein kinase Akt2 (PBK beta). *Science*. 2001;292:1728-1731
2. Daugherty A, Manning MW, Cassis LA. Angiotensin II promotes atherosclerotic lesions and aneurysms in apolipoprotein E-deficient mice. *J Clin Invest*. 2000;105:1605-1612
3. Daugherty A, Manning MW, Cassis LA. Antagonism of AT2 receptors augments angiotensin II-induced abdominal aortic aneurysms and atherosclerosis. *Br J Pharmacol*. 2001;134:865-870
4. Shen YH, Utama B, Wang J, Raveendran M, Senthil D, Waldman WJ, Belcher JD, Vercellotti G, Martin D, Mitchelle BM, Wang XL. Human cytomegalovirus causes endothelial injury through the ataxia telangiectasia mutant and p53 DNA damage signaling pathways. *Circ Res*. 2004;94:1310-1317
5. Shen YH, Zhang L, Gan Y, Wang X, Wang J, LeMaire SA, Coselli JS, Wang XL. Up-regulation of PTEN (phosphatase and tensin homolog deleted on chromosome ten) mediates p38 MAPK stress signal-induced inhibition of insulin signaling: A cross-talk between stress signaling and insulin signaling in resistin-treated human endothelial cells. *J Biol Chem*. 2006;281:7727-7736
6. Li XN, Song J, Zhang L, LeMaire SA, Hou X, Zhang C, Coselli JS, Chen L, Wang XL, Zhang Y, Shen YH. Activation of the AMPK-FOXO3 pathway reduces fatty acid-induced increase in intracellular reactive oxygen species by upregulating thioredoxin. *Diabetes*. 2009;58:2246-2251

Supplemental Table, Figures, and Figure Legends

Online Supplemental Table I. Patient Characteristics

Characteristics	Control (n=12)	TAA (n=12)	TAD (n=16)
Age (yrs)	61.3±7.1	66.8±4.7	63.6±5.1
Male sex	3 (33%)	5 (42%)	13 (72%)
History of smoking	4 (33%)	11 (92%)	12 (67%)
Hypertension	8 (67%)	10 (83%)	17 (94%)
Diabetes mellitus	5 (42%)	2 (17%)	0
Stroke	4 (40%)	1 (8%)	2 (11%)
Aneurysm diameter at sample site (cm)	N/A	6.2±1.1	6.5±1.0

TAA, thoracic aortic aneurysm; TAD, thoracic aortic dissection; N/A, not applicable.

Data are expressed as number and proportion or mean ± standard deviation.

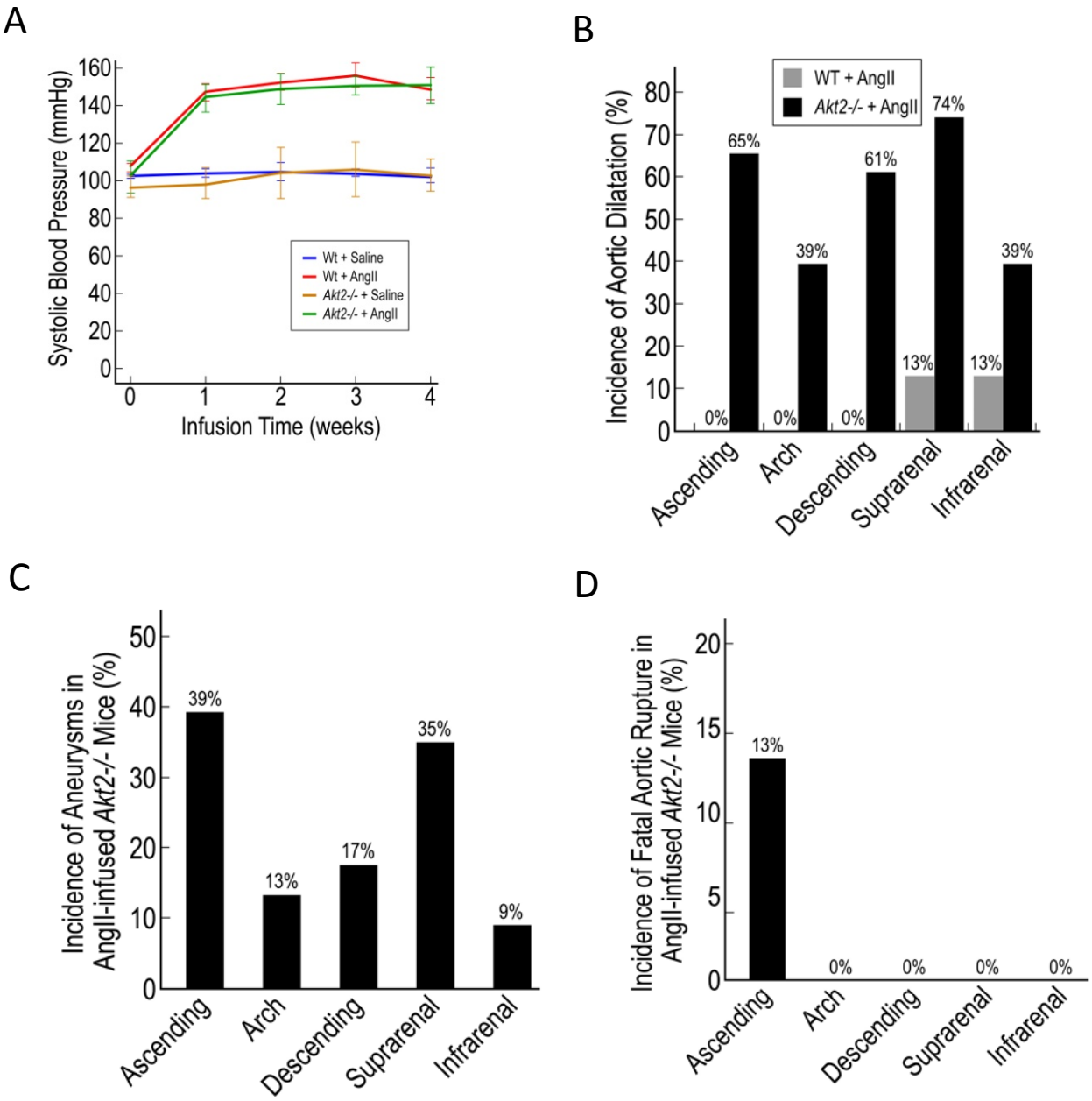

Online Supplemental Figure I. Development of aortic aneurysms and dissections in *Akt2-/-* mice infused with AngII. WT and *Akt2-/-* mice were infused with saline or angiotensin II (AngII) for 4 weeks. (A) Increases in systolic blood pressure in wild-type (WT) and *Akt2-/-* mice challenged with AngII were similar. The incidence of (B) aortic dilatation, (C) aneurysm, and (D) fatal rupture that occurred in AngII-infused *Akt-/-* mice is shown according to the aortic segment involved.

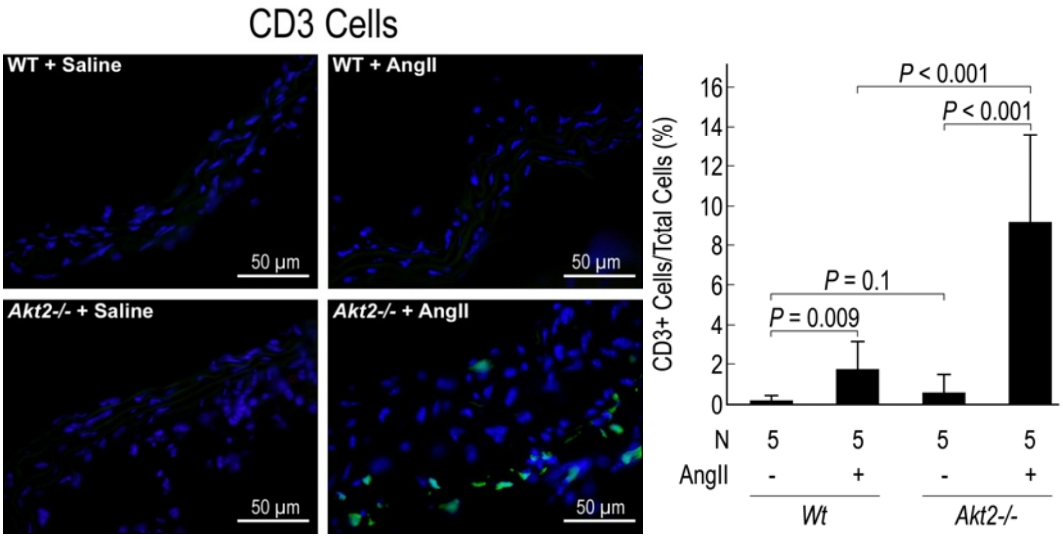

Online Supplemental Figure II. CD3 T cells were significantly increased in the aortas of AngII-infused *Akt2-/-* mice. Representative images of immunofluorescence staining and quantification (mean positive staining area normalized with evaluated aortic area) of CD3-positive cells in the aortic wall.

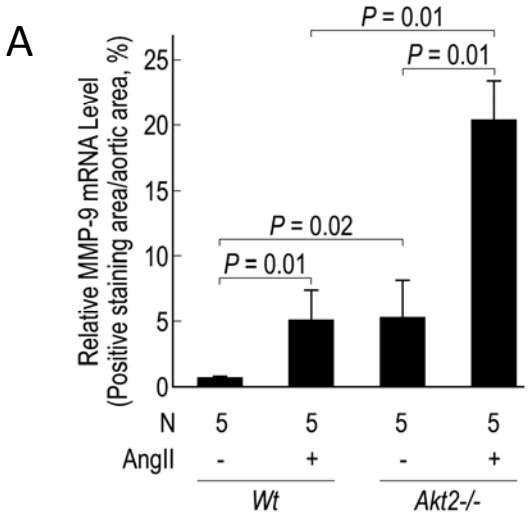

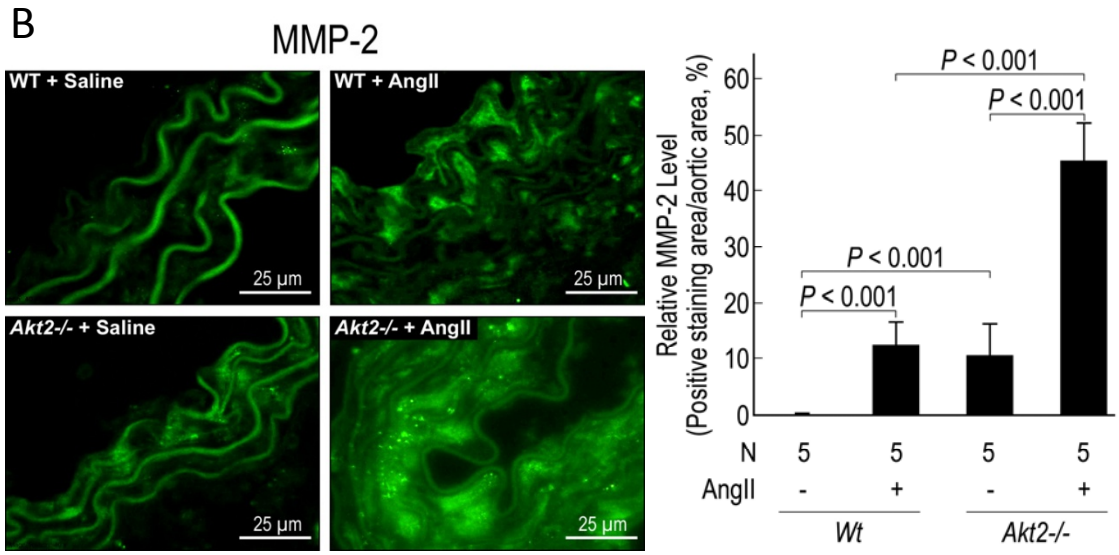

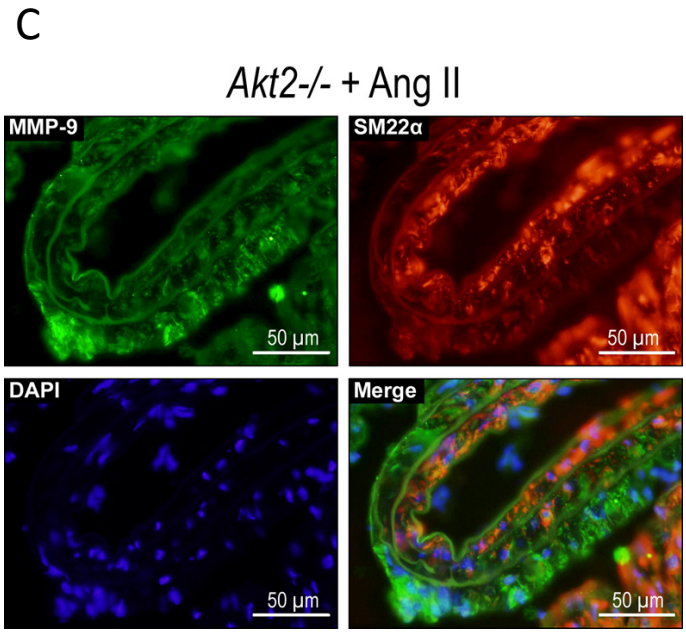

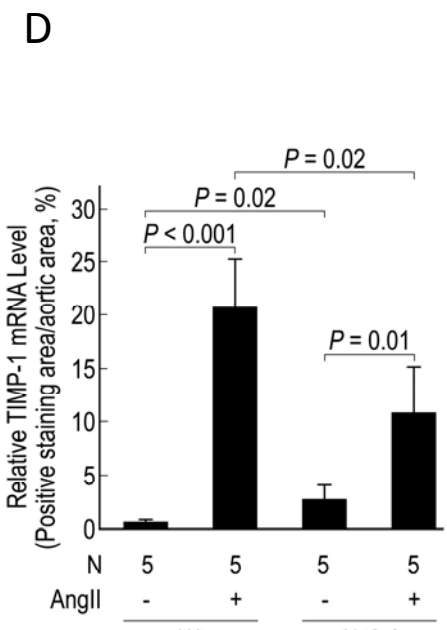

E

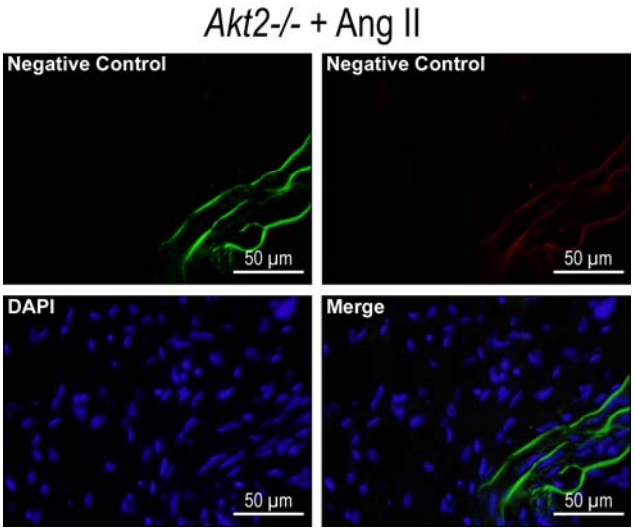

Online Supplemental Figure III. Significantly increased MMP expression and MMP-9/TIMP-1 ratio in AngII-infused *Akt2-/-* mice. (A) Quantitative real-time PCR analysis of *MMP-9* mRNA showing increased MMP-9 expression in aortas from AngII-infused *Akt2-/-* mice. (B) Representative images of immunofluorescence staining and quantification (mean positive staining area normalized with the evaluated aortic area) of MMP-2 in the aortic wall. (C) Double staining for MMP-9 and SM22α shows increased MMP-9 expression in SM22α-positive SMCs in the aortas of AngII-infused *Akt2-/-* mice. (D) Quantification of TIMP-1 expression (the mean positive-staining area normalized with the evaluated area) shows lower TIMP-1 expression in aortas from AngII-infused *Akt2-/-* mice than in AngII-infused WT mice. (E) Representative negative control for double staining of aortas from AngII-infused *Akt2-/-* mice.

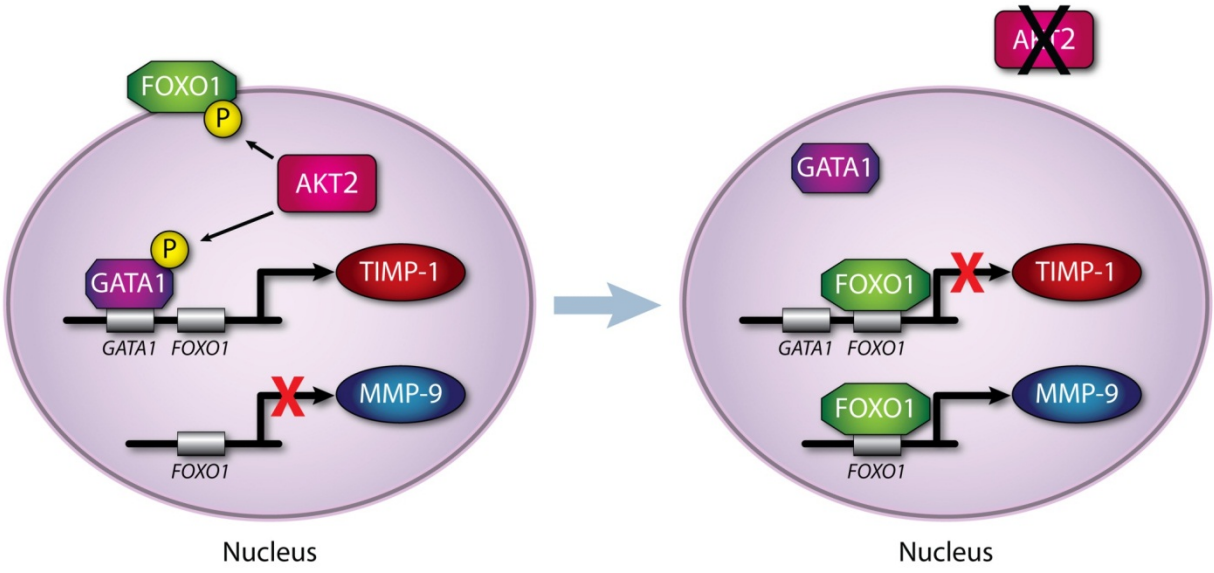

Online Supplemental Figure IV. A model for the AKT2-mediated regulation of MMP-9 and TIMP-1 expression in the aorta. In the presence of AKT2 (left panel), phosphorylation of FOXO1 by AKT2 excludes FOXO1 from the nucleus. The phosphorylation of GATA1 by AKT promotes GATA1 binding to the *TIMP-1* promoter and *TIMP-1* transcription. In the absence of AKT2 (right panel), unphosphorylated FOXO1 translocates into the nucleus and binds to the *TIMP-1* promoter, thus preventing GATA1 binding to the *TIMP-1* promoter and *TIMP-1* transcription. In contrast, unphosphorylated FOXO1 in the nucleus binds to the *MMP-9* promoter and promotes *MMP-9* transcription.